EXTREME TEMPERATURE & AIRWAY SMOOTH MUSCLE CELL DEATH

Effects of Extreme Temperature on Airway Smooth Muscle Cell Death:

Insights into the effects of bronchial thermoplasty on airway smooth muscle

By

Lindsay DoHarris, BScH SSP

A Thesis Submitted to the School of Graduate Studies

In Partial Fulfillment of the Requirements

For the Degree Masters of Science

MASTERS OF SCIENCE (2011) McMaster University

(Medical Sciences: Physiology and Pharmacology) Hamilton, Ontario

TITLE: Effects of Extreme Temperature on Airway Smooth Muscle Cell Death

AUTHOR: Lindsay DoHarris, B.Sc.H, SSP (Queen's University)

SUPERVISOR: Dr. Luke Janssen, Ph.D.

NUMBER OF PAGES: x, 93

Abstract

Bronchial thermoplasty has recently been FDA approved as a novel therapy for use on adults suffering from severe asthma. The procedure uses radiofrequency energy to heat the airways to 65°C for 10 s. This has been shown in dogs to lead to a reduction of airway smooth muscle mass and in humans to improve quality of life and asthma control. Early cellular reactions to this treatment are unclear; as well, there is limited information regarding thermal sensitivity of airway smooth muscle when exposed to extreme temperatures (50-65°C). We examined the cellular impact of bronchial thermoplasty by investigating the response of airway smooth muscle to heat by immersing bovine tracheal strips and bronchial segments in heated Krebs. We confirmed dramatically decreased functionality over the temperature range 50-60°C at 1 h and 24 h in all tissues. TUNEL analysis noted significant cell death in all tissues heated to 65°C and limited cell death in bronchial tissues treated with <55°C. Immunohistochemical analysis showed an effect of temperature on caspase 3 activation in bronchi; tracheal strips demonstrated co-localization of caspase 3 and TUNEL at 55°C but not 65°C. These data suggests that cell death of airway smooth muscle contributes to the cellular effects observed following heating to 65°C; at lower temperatures, cell death may be limited. We conclude that bronchial thermoplasty (heat treatment to 65°C for ~30 seconds) leads to a number of structural and functional changes in the airway smooth muscle, which culminate in marked loss of function and cell death.

Acknowledgements

Reflecting on this process of completing a Master's thesis, there are many people who have helped along the way, providing support and guidance. Here, I would like to acknowledge a number of people that contributed directly or indirectly to this finished product.

I would first like to thank my supervisor Dr. Luke Janssen who has been a fantastic mentor and teacher throughout this project. I truly appreciate all the time you spent ensuring my understanding of smooth muscle dynamics, keeping the project moving forward and also for supporting me financially as a member of your lab. As well, thank you to my committee members Dr. Mark Inman and Dr. Gerard Cox for their invaluable input and advice.

I have relied on several colleagues for help with data collection and research techniques. Specifically, Tracy Tazzeo an expert with the muscle baths who also spent many hours counting slides; Sarka Lhotak who has answered many a question about staining; Russ Ellis who initially taught me protocols for staining and counting cells; as well, Katherine Radford, Brent Humber, Dr. Dusan Lukic, Dr. Tariq Aziz, Amanda Giesler and Nirooya Siva have all lent assistance when needed.

I am grateful to my parents, brother and grandparents who have been encouraging and supporting me for my entire life in every pursuit. Having a supportive and loving family is a blessing - without your guidance I would not have gotten anywhere in life. I appreciate beyond words the material and immaterial help of Shyam Maharaj; you have been a rock with kindness, encouragement and advice through both good and tough times. I will also express my gratitude to Buddha Shakyamuni and the Samudra Centre for spreading Dharma and providing spiritual support.

To any colleagues, family or friends who were not mentioned by name, I thank you for your support and appreciate the contributions you made to help with the completion of this thesis.

Table of Contents

List of Figures with Description

List of Abbreviations

- ASM – Airway Smooth Muscle
- AQLQ – Asthma Quality of Life Questionnaire
- ECM – Extracellular Matrix
- FEV_1 – Forced Expiratory Volume in one second
- H&E – Hematoxylin and Eosin
- RF - Radiofrequency
- TUNEL – Terminal deoxynucleotidyl transferase UTP Nick End Labeling

Introduction

General Introduction

Asthma is a common chronic respiratory condition which affected over 2.3 million Canadians in 2009 [1]. The condition is associated with reversible airflow obstruction which is commonly referred to as an asthma attack. The economic impact is measured in billions of dollars to account for lost days from work, doctor's visits and hospitalizations. Current drug therapies, namely beta agonists and corticosteroids, are able to treat exacerbations and provide temporary relief

for asthma sufferers but are unable to halt the progression of the disease or provide lasting relief to people that suffer from asthma.

A novel therapy has recently been introduced to address this need for long term improvement of the asthmatic condition. This therapy uses heat delivered directly to the bronchial wall and seeks to ablate the smooth muscle and thus eliminate the excessive bronchoconstriction causing asthma attacks. The procedure met with numerous trials to demonstrate efficacy and safety; however it is not clear what molecular mechanisms achieve this goal.

This study uses a thermal model to investigate whether the temperatures that smooth muscle is subjected to during bronchial thermoplasty can reasonably account for the physiological benefit of this procedure. Specifically, we will observe the effects of extreme temperatures for durations mirroring the clinical setting on the contractility and viability of smooth muscle tissue.

Asthma Diagnosis and Classification

Asthmatic symptoms are associated with exposure to a trigger which induces reversible airflow obstruction. Potential triggers include allergen exposure[2,3], exercise[4] and pollution [5]. A continuum for classification of disease severity has been established with regard to FEV_1 (forced expiratory volume in 1 second) and the medications required to manage an individual's symptoms. The

disease is classified as mild, moderate or severe along with designations of controlled or uncontrolled - according to the type and dosage of medication required to achieve control. The Canadian Thoracic Society consensus guidelines were established to standardize asthma diagnostics on this basis[6].

FEV_1 and PC_{20} (concentration required to cause a 20% decrease in FEV_1) are reliable measurements that assist with the diagnosis and classification of asthma[7]. For these measures, patients will exhale forcibly from total lung capacity and volume at 1 s will be recorded, methacholine can then be administered at elevating doses to note the point at which FEV_1 decreases by 20% [7]. Depending on the measured outcomes (FEV_1, PC_{20} as well as the level of control achieved by the use of medications the individual receives) a diagnosis is produced [6-8]. Another tool, the asthma quality of life questionnaire (AQLQ), was developed to create a measure that would reflect the impact of interventions on the lives of adults with asthma. This has since been used as a tool to assist with clinical trials and evaluates environmental effects, emotional dysfunctions and impairment of normal activities[9,10].

Pathophysiology of Asthma

Airway remodeling and chronic inflammation are hallmarks of asthma that underlie the airway hyperresponsiveness. Behind these symptoms is a complex

interaction between the immune system and airway wall. Airway smooth muscle (ASM) can stimulate the recruitment of immune cells and immune cells can in turn stimulate ASM to proliferate thus sparking a reciprocating pattern. FEV_1 measurements in asthmatics can be improved through the use of corticosteroids; however in the majority of cases measurements are still far from the norm and structural changes are suggested to underlie this difference[11, 12]. A treatment is thus needed to address structural abnormalities present in asthmatic airways.

Remodeling

Remodeling of the airways includes hyperplasia or hypertrophy of ASM as well as increased collagen deposition and heightened levels of alpha smooth muscle actin [3,13,14] (see section *Airway smooth muscle in asthma*). Combined, these factors increase the thickness of the airways in persons with asthma.

It is clear that increased thickness of the airway wall correlates with asthma severity [2,15,16]. In mild asthmatics airway wall thickening has begun, however this may be a reversible change which becomes permanent through repeated exacerbations and chronic inflammation [12,16]. As well, structural remodeling correlates with FEV_1, indicating a direct connection with respiratory effects [15,16]. The evidence of airway remodeling does not differ between atopic and non-atopic asthma [2] and ASM as a component of the airway wall is

increased in asthmatics [14]. While inflammatory mediators ameliorate excess inflammation present in the airways and hyperresponsive effects are improved by the use of bronchodilators, there is no treatment that targets thickening of the airway wall.

Smooth Muscle

Smooth muscle tissue is found in the airways, gut and blood vessel walls. Peristaltic force generated by the smooth muscle is helpful in the gut to aid in digestion and contraction in the blood vessels helps with circulation and tone of the circulatory system. It is unclear the role that ASM plays in the lungs; however, in diseased airways smooth muscle dysfunction plays a major role through excess bronchoconstriction, increased mass and interactions with the extracellular matrix (ECM)[17].

Airway Smooth Muscle in Asthma

In asthma, airway remodeling includes alterations of airway wall components, quantity and function of cells. Alterations in the basement membrane potentially include hyperplasia/hypertrophy of smooth muscle, improper adaptation to length changes, altered ECM deposition, and/or altered

contractile properties of smooth muscle tissue [18]. One or a combination of these factors would result in excessive ASM shortening and thereby excessive airway narrowing as seen in asthma [14,18].

The ASM mass in severe asthmatic airways is increased relative to normal controls[14,19]. This on its own may explain excessive narrowing by a simple association of increased mass with increased volume of tissue causing further narrowing of the lumen or increased contractile force of muscle decreasing the airway diameter[20]. There remain questions about whether the mass is due to hypertrophy or hyperplasia of smooth muscle cells and what causes this increase (inflammatory reaction, ECM, etc.). ECM components, collagen and elastin, or stimulation by inflammatory cells may influence proliferation and survival of these cells[21].

The ECM may also play a role in the dysfunction of ASM through altered composition[19] or a reciprocal relationship. Specifically, ASM produces ECM proteins as well as matrix metalloproteinases and tissue inhibitors of metalloproteinases. The balance of these proteins controls breakdown and composition of ECM; meanwhile, ECM may modulate the survival, proliferation and cytokine production of ASM[21].

Attempts are being made to intervene in the hyperactive signaling pathways via signal transduction, calcium release, or the contractile mechanism. While understanding of ASM contractile function is rapidly increasing, headway

towards a novel intervention in this area has been challenging likely because of the complex interactive machinery that is behind disease symptoms [22].

Contractile mechanism

Contractile proteins in ASM have a dynamic structure of myosin and actin that is capable of generating optimal force from various lengths[23,24]. The dynamic structure involves myosin which is able to disassemble and reassemble allowing length adaptation [25]. Contraction can be stimulated by an influx of calcium from extracellular or intracellular stores or an agonist which then enacts a cascade of proteins to cause phosphorylation by myosin light chain kinase; relaxation of myosin is stimulated by dephosphorylation by myosin light chain phosphatase[26]. In an animal model of asthma, varied myosin isoforms or expression of contractile signaling proteins can account for greater force and faster contractile action seen in Fisher rats and this may also be an underlying mechanism of hyperresponsiveness in humans[27].

Also involved in contraction are small heat shock proteins, HSP20 and HSP27[28]. HSP27 has been shown to have a role in contraction of some agonists as regulated by phosphorylation and to co-localize in areas of crossband formation along with actin and other contractile proteins [29]. HSP20 as well has been shown to promote relaxation of ASM when phosphorylated [30]. These

proteins are thought to act through the regulation of actin polymerization, HSP27 promoting and HSP20 preventing filament formation; this would be supported by additional effects of small heat shock proteins on cell adhesion and stress fibre formation [31,32] .

In normal cells, HSP27 is minimally expressed and will become upregulated following a variety of stressful events such as loud noise, UV or heat exposure[31,33,34]. When up-regulated, HSP27 plays a role in resistance to cell stress and can inhibit apoptosis[32]. This is done by preventing the formation of insoluble aggregates from unfolded proteins within the cytoplasm after disruptive events like increased heat or oxidative stress [35,36]. Increased expression of small heat shock proteins plays a role in the stress tolerance exhibited by cells pre-treated with a sub lethal dose of heat. And, the constitutive expression of small heat shock proteins in smooth muscle cells may give additional protection to stress events.

Purpose

It is apparent that ASM is a potential player in asthma; however it is only recently that the normal physiological role has been questioned. It remains unclear what function ASM has in a normal human but there are several credible suggestions. These would include a peristaltic role in cough/ mucus clearance, a

protective barrier or a role in development [37,38]. With the exception of a developmental role, these and other suggestions have been largely discounted in the literature[17,39]. A compelling argument has been established to suggest that development of the lungs requires ASM for development and branching[40-42]. Such a role would not deter from the positive effects of tissue ablation. Backing up this claim are safety studies following the ablative process of thermoplasty that shows no significant safety effect following application of radiofrequency (RF) heat [43-47](see section on *Bronchial Thermoplasty*).

Bronchial Thermoplasty

Bronchial Thermoplasty was introduced in 2004 by Cox *et al* [48], as a novel treatment for asthma. This procedure sought to target the smooth muscle directly through radiofrequency ablation and assumed both that ASM is a vestigial tissue and that treatment focusing on smooth muscle alone is enough to improve asthmatic symptoms. Bronchial Thermoplasty is a technique that has been shown in clinical trials to alleviate asthmatic exacerbations and improve AQLQ scores following the application of heat to airway walls [46]. Despite FDA approval of this technique, controversy still surrounds the use of thermoplasty [49,50].

Procedure

The bronchial thermoplasty procedure utilizes an expanding basket introduced by bronchoscopy to heat the airways with RF energy. The Alair system (Asthmatx, Mountain View, CA) includes a bronchial catheter and RF generator. The catheter extends through a fibre optic bronchoscope where the tip, an expanding four pronged basket, protrudes and expands to contact the airway wall. The RF generator then produces 460kHz [51,52] and a feedback mechanism maintains the temperature at ~65ºC for 10 seconds before the basket is moved to an adjacent location [51,52]. The treatment requires three visits of approximately 1 hour scheduled three weeks apart to complete; first targeting the lower right lobe, the next targets the lower left lobe and finally both upper lungs. The patient will be placed under moderate sedation for the procedure and sent home the same day after a normal assessment of breathing rate, blood pressure, heart rate, lung function and blood oxygen levels [53,54].

Clinical Trials

Several trial groups have undergone the thermoplasty procedure and experienced positive results. An initial prospective study involved 9 patients undergoing preoperative bronchoscopy during which they received the bronchial

thermoplasty treatment. This area was resected during lobectomy 1-3 weeks later and examined. There were no adverse clinical effects visible beyond reddening and edema of the mucosa; as well, H&E staining indicated a reduction of ASM [55]. A second feasibility trial involving 16 patients was performed that indicated safety of the procedure and positive results including decreased hyperresponsiveness[56].

Three larger trials followed the feasibility studies all of which found improvements in AQLQ scores. The AIR trial was able to demonstrate safety in mild-moderate asthmatics and a follow-up with these patients demonstrated long term safety of the technique[43,57]. The RISA trial then indicated the procedure was safe and effective in severe asthmatics[47]. A large, randomized multi-centre AIR 2 trial followed these to examine on a large scale the efficacy of the treatment for persons with severe asthma. Improvements in the AIR 2 trial included a reduction in ER visits, fewer days off work, an improved AQLQ score and fewer severe exacerbations were experienced by patients in the post-treatment period[46]. A meta-analysis of these trials pooled data from 421 patients and confirmed findings of AQLQ improvements and further noted peak expiratory flow increased[45].

Adverse events were increased as a result of the procedure; however these mainly occurred within a day of the treatment and cleared within a week; there was no increase over sham treated subjects during the post-treatment

period[45]. Adverse events included wheezing, coughing, discoloured sputum and chest discomfort and hospitalizations increased during the treatment period[44,45].

Bronchial thermoplasty received Federal Drug Administration approval in the US in April of 2010[44]. It is available for use on individuals over 18 who have severe persistent asthma which is not adequately controlled by inhaled corticosteroids and long-acting-beta-agonists[53,58].

Mechanisms of Bronchial Thermoplasty

There were few preclinical experiments published regarding the molecular mechanisms behind the bronchial thermoplasty procedure. This is likely due to the strong positive outcome observed in dogs and the ready human model with lung biopsy used in the feasibility studies[55]. Experiments that were carried out in dogs were able to demonstrate a reduced response to methacholine challenge following heat application which persisted for three years[59]. These studies also showed no charring of surfaces but did note a change in morphology centering on the smooth muscle, which was replaced by loose connective tissue [48]. Prior to human application, temperatures and durations were varied to promote optimal effectiveness - minimal destruction of tissue that results in ablated response.

Since then, experiments have focused on the physiological effect of heat treatment in canines. Effects on airway closure and distensibility were measured

and found to decrease when heated[60]. As well, Brown and colleagues[61] found that airway diameter can contribute to asthmatic symptoms, which is supported by a decrease in baseline airway diameter in dogs following heating[59].

Computational models have also been developed to depict heating assuming particular parameters of size, conductivity heat capacity, etc. These assume an airway diameter of 2-8 mm and airway wall thickness at 10% of diameter. There were minimal changes in temperature conductance as the model parameters of thickness and diameter were altered. Results suggest the airway wall will reach a temperature approaching 65ºC, however it is not clear what effect this temperature has on the tissue involved [51].

Temperature sensitivity of the ASM was directly investigated by Dyrda *et al*[62]. Here, a heating model was used whereby the tissue was dissected and immersed in Krebs buffer for a period of ~30 s. With these studies the effects of temperature on upstream signaling proteins (myosin light chain kinase, TRP channels) were discounted and it was noted that the temperature sensitivity of myosin corresponds with the heat at which functionality is decreased in these tissues. Thus, denaturation of the myosin protein has been implicated as part of the molecular effects of bronchial thermoplasty[62]. Myosin plays a key role in contraction with ATP dephosphorylation leading to conformational changes that produce a power stroke detaching and subsequently binding to an upstream

location on the actin filament. Stability of the myosin filament and susceptibility to thermal energy is dependent on the contractile state of the myosin filament [63].

Remaining Questions

Much of the remaining uncertainty surrounds the cellular effects that result in a successful treatment. Safety, efficacy and improved quality of life have been demonstrated and the only reproducible physiological change demonstrated in humans thus far is an increase in peak expiratory flow [45] . The suggested beneficial mechanism is reduction of smooth muscle mass[55], however this has only been investigated in humans during feasibility trials and improvements in FEV_1 measures have not been observed[45], which would be expected to correlate with airway wall thickness and ASM mass (see *Pathophysiology of Asthma - Remodeling*).

The suggestion of ASM mass reduction is based on early evidence showing decreased ASM in dogs and reduced responses to methacholine challenge[55,59]. A relationship between extreme heat exposure and acute force measurements in ASM has already been demonstrated, suggesting that the myosin is disrupted following heating[62]. This contractile protein is important in force production [26,64]; however, other effects of this extreme temperature are

unclear. More clarity is needed surrounding this topic to alleviate concerns and potentially counter early adverse effects.

Temperature Effects

Radiofrequency energy will produce cellular effects by generating heat. The general effect of heat on the cell is to cause protein unfolding and exposure of hydrophobic residues, producing aggregation of said proteins [65]. Cellular changes associated with the increased temperature include alterations in membrane permeability, disruption of metabolic processes and disruptions of the nucleus. Damage to the nucleus is central to the cell killing effects of heating [66,67]

Generally speaking, unfolded proteins within a cell will stimulate the heat shock protein response and when this process is overwhelmed the cell will undergo organized apoptosis. However, if damage is too great the cell will be unable to begin an organized process to promote survival or initiate cell suicide so in its inability to function, it will become necrotic. Coagulative necrosis describes the process where the number of denatured proteins interferes with cellular processes to result in pathologic cell death[68].

Radiofrequency Ablation

Radiofrequency ablation produces heat through friction by causing rapid rotation of polar molecules, such as water[69]. The high water content of biological tissues enables good conductivity; this is decreased in airways which have a higher resistance[69]. The airway wall is suggested to be 10% of the diameter, which would place the airway wall <1 mm from the heat source. Previous models of RF conductivity lead us to believe that following the procedure the smooth muscle layer will have reached a temperature approximating 65°C [51,70,71].

There are a range of RF devices currently being used for ablative treatments, most commonly cancer treatments [69]. Because of this and previous concerns regarding cellular phones and microwaves, the safety of non-ionizing RF energy has been established. Bronchial thermoplasty, which is on the lower end of the spectrum, uses 460 kHz and is considered safe. Damage that results from application is due primarily to heat conducted into the airway walls [72].

RF energy is currently used to ablate tumors. When this technique is applied, a zone of coagulation is visible that corresponds to heating of the tissue to a temperature of approximately 65°C within which macroscopic tissue appears white[68,73]. Microscopically for a short time following, cells retain a normal appearance and are termed ghost cells, meaning that under Hematoxylin & Eosin staining the nuclei are light compared to the unablated tissue zone but the cells

otherwise appear normal[74]. This can be referred to as coagulative necrosis due to the coagulation of proteins within the cells. A similar phenotype and ghost cell are visible following ischemia.

Cellular Response to Heating

Temperature is the major determinant of the cellular response to heat. Every protein has a transition temperature at which bonds will be disrupted to deform the structure and effect the functioning of said protein. Thermal transitions can be measured by differential scanning calorimetry which pinpoints the temperature and energy input required for denaturation. A single protein may have several transition points indicating that stability of different sections varies. A minority of proteins are able to renature when cooled, indicating that they do not require assistance to reacquire their functioning form. When denatured, proteins will form insoluble aggregates within a cell.

Chaperones are present in all cells and are involved in the unfolded protein response assisting with refolding of proteins or preventing aggregation. The chaperones involved in this reactive process to heating are referred to as heat shock proteins. There are several types classified by their molecular weight and these may interact differently within the cell. Large heat shock proteins, HSP70 and HSP90, are able to use ATP to assist with refolding of damaged

proteins whereas HSP27 and HSP22 are small heat shock proteins which can assist only with sequestration but function to higher temperatures[75].

The small heat shock proteins are of particular interest when studying heat sensitivity in smooth muscle because these also play a role in contraction through stabilization of actin filaments [28] (see *Smooth Muscle: Contractile Mechanism*). Because of this, there is likely a higher physiological concentration of HSP27 in smooth muscle tissue. Interestingly, increased levels of HSP27 were shown to increase survival of smooth muscle cells at hyperthermic temperatures [76,77] and over expression in other tissue types has a similar effect [32,34]. HSP27 has a protective effect on cells by blocking apoptosis [32] and stabilizing aggregation of denatured actin[78-80]. Additionally, HSP27 is able to reversibly denature allowing it to function after cooling or at temperatures where large heat shock proteins are unable to[75].

Temperature Profiles

Cell death will occur in a time and temperature dependent manner. Most studies to date have investigated temperature effects when heated to hyperthermic temperatures (up to 45°C) for a time period of 15 min to 1 h. In these cases, most cell death will occur by apoptosis or mitotic catastrophe following nuclear disruptions[65]. At temperatures between 40°C and 46°C, heat

shock proteins will act as chaperones and attempt to repair damage caused by protein unfolding and aggregation[65]. Activation of apoptotic proteins Bcl-2 and Bax by caspase 2 is temperature sensitive and their activation will lead to cell death[81,82].

At temperatures beyond 45°C when cell cultures are heated for over 1 h, cell death is observed to become primarily necrotic as opposed to apoptotic[83,84] the specific temperature required to initiate cell death can change slightly based on cell type[83,85] and tissue[73]. In prostate cells heated for less than 5 minutes, mechanics of cellular injury were observed to change at 54°C with an increase in HSP27 expression following heating still evident at 56°C when treated for 1 minute[34]. Interestingly, when cells are thermally damaged, an active bystander effect in which the viability of non-treated, neighbouring cells is affected has been noted to occur in certain situations following heating[86]. Lepock and colleagues [87]have observed that at temperatures above 70°C DNA will be denatured and have correlated a potential critical protein target for killing cells and thermal radiosensitization with the nuclear matrix component denatured in transition I of DSC profiles, approximately 51°C. The temperature range relevant to this project is 50-65°C. At this temperature, components of the nucleus, nuclear matrix [66,87] or myosin [88,89] may be affected.

Differential scanning calorimetry profiles have demonstrated the various transition points of nuclear and cellular proteins[88,9087]. Studies have also shown

that large heat shock proteins are not active and that myosin is dysfunctional in ASM at extreme temperatures[62]. Other studies confirm the denaturation of myosin at temperatures nearing 55°C [63,88,89]and aggregation of myosin was observed to maximize between 56°C and 58°C[89].

Heating tissues prior to a variety of insults will increase survival/decrease injury of tissue, likely by increasing the availability of heat shock proteins[83]. Involved in this process is HSP27, which acts to block mitochondrial independent pathways of apoptosis induced by $CoCl_2$ (this mimics processes caused by hypoxia or ischemia) as well as intrinsic apoptosis[32]. Small heat shock proteins are upregulated following the initial insult and effects thermal denaturation and the aggregation of F-actin[79]. HSP27 has been shown to prevent aggregation but not denaturation of both myosin and actin [35,79]. This is done by forming soluble complexes with denatured proteins, thus protecting the cytoskeleton from disruption by large insoluble complexes [78]. The activity of HSP27 has been shown to have a protective effect both in vitro when guarding against hypoxia [32]and in vivo associated with vascular disease[80].

Cell Death

Cell death can be broadly categorized as a programmed physiological process or a pathologic consequence of injury: apoptotic or necrotic. Among

these broad headlines are also autophagy, coagulation necrosis, mitotic catastrophe, etc. Heating of tissues has been shown previously to lead to heat shock response, apoptosis, necrosis or coagulative necrosis depending on the temperature achieved.

During apoptosis, excessive cell stress or induction of a signaling cascade will cause mitochondrial release of cytochrome c into the cytoplasm that interacts with Apaf-1 to form an apoptosome[91](Fig. 1). The apoptosome then initiates cleavage of initiator and effector caspases to induce cell death mechanisms. The apoptotic process will proceed over several hours and result in DNA cleavage at lengths of 180-200 base pairs and membrane blebbing which retains cytoplasmic components from exposure preventing a damaging inflammatory response.

Necrosis is a pathologic process where the membrane is disrupted and the cytoplasmic contents of the cell are released causing an inflammatory response. Necrosis results from severe damage to a cell that renders it unable to undergo the apoptotic process.

Following radiofrequency ablation in cancer cells or ischemia, the resulting death that is hallmarked by ghost cells is termed coagulative necrosis [92,73,93]. This denotes a cell which contains a coagulated morphology, sometimes termed ghost cells due to the lightened appearance of nuclei which persists for a few days. During this period the area of necrosis appears white and may be followed by reddening of tissue caused by an inflammatory response. The necrotic tissue will

either be replaced or scarring will result as fibroblasts are recruited to the area. Similar to coagulation necrosis is liquefactive necrosis where cells or tissue have a high concentration of lipids or inflammatory cells whose death releases enzymes that break down tissue[92].

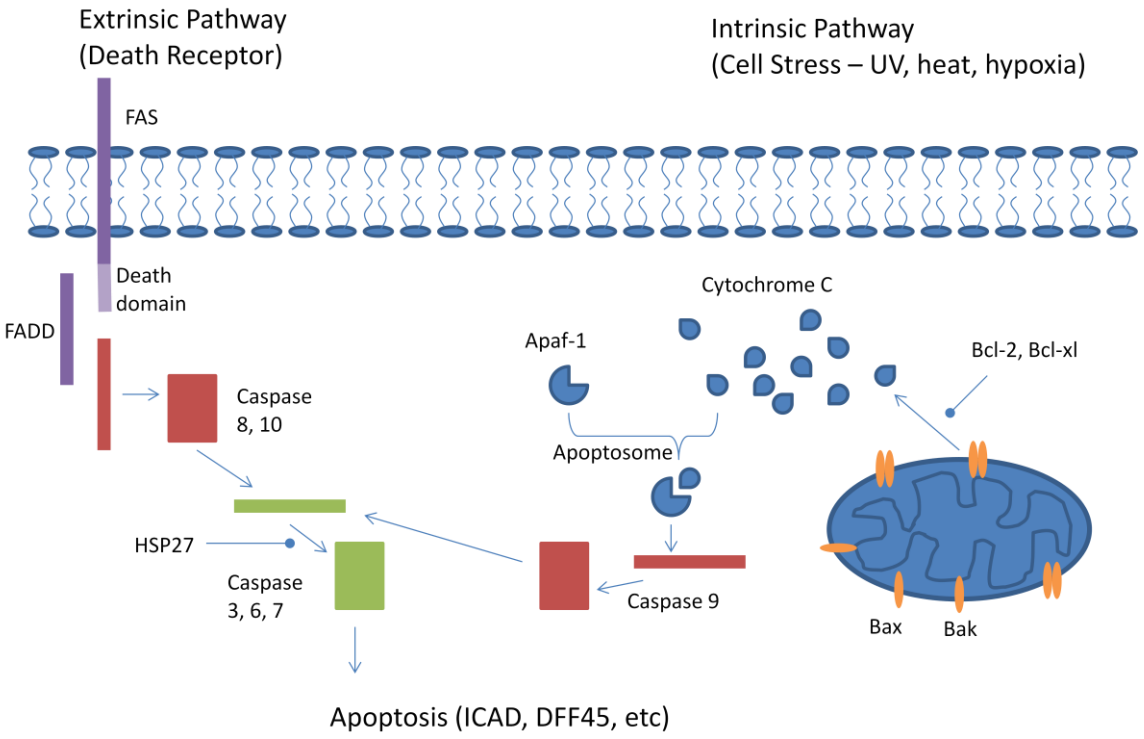

Figure 1. Apoptosis can occur via an extrinsic or intrinsic pathway. The extrinsic pathway is initiated by a ligand binding to a transmembrane FAS receptor which contains a death domain on the interior. FADD can then bind to this death domain and cause the cleavage of pro-caspase 8. Active/Cleaved caspase 8 will cleave pro-caspase 3 to commence activity of caspase 3 and, in turn, apoptotic processes. Intrinsic apoptosis is initiated in the mitochondria as a result of cellular stress (hypoxia, UV exposure, etc.) cytochrome c is released into the cytoplasm and associates with apaf-1 to cleave initiator caspases which in turn activates effector caspases to commence apoptosis. Throughout this pathway, several proteins act to inhibit its progress including BCL-2, BCL-xl and heat shock proteins.

Detection of Cell Death

Detection of cell death should include multiple markers[94,95]. A common and reliable method to detect cell death is using a terminal deoxynucleotidyl transferase UTP nick end labeling (TUNEL) stain accompanied by active caspase 3 [96,97]. The TUNEL will label the 3' hydroxyl ends of DNA indicating one of the final stages of apoptotic cell death has been completed. This method alone is not sufficient to determine apoptotic cells as necrotic cells may also nonspecifically stain for cleaved DNA [95,94]. Active caspase 3 is used to observe/confirm apoptosis through quantification or fluorescence co-labeling. It is important to note that caspase 3 occasionally plays a role in other processes such as autophagy so on its own does not define dead cells [98]. As such, juxtaposition of caspase with TUNEL using fluorescence or quantification is needed to conclusively indicate apoptosis is occurring.

Cell death following heating has been measured to increase over time and plateau [83]. Following heating, caspase activity has been measured between 1-24 h and TUNEL is evident at 1-24 h following heating [83,84,96]. Time points at the beginning and middle/end of the process will give an indication of cell death that occurred.

Experimental Hypothesis and Objectives

It is important to understand more about the cellular mechanisms behind the bronchial thermoplasty procedure. The effect of heating smooth muscle tissues to an extreme temperature for this duration has not previously been investigated and this knowledge is vital to enable directed improvements/modifications of the thermoplasty procedure or to correct unforeseen obstacles. Knowing the cellular reaction of smooth muscle can allow prevention or better treatment of adverse events that follow the procedure in the first 24 h. As well, this information may stem controversy around the use of thermoplasty by supporting the suggestion that smooth muscle ablation is behind the positive effect of the treatment.

Hypothesis

We hypothesize that exposure to temperatures of 55°C and 65°C for 30 s – 1 min will result in structural/cellular reorganization, response mechanisms and/or damage of ASM. We think these changes include decreased functionality in these tissues and cell death via apoptotic or necrotic mechanisms.

We will address these hypotheses by confirming contractile effects previously noted[62], by investigating phenotypic presentation and DNA cleavage,

and by identifying apoptotic protein activation following immersion in heated medium.

Experimental Design

We have used a model of bovine ASM immersion in heated Krebs buffer to demonstrate the molecular effects of short duration exposure to extreme temperatures. This is primarily of interest as a model of bronchial thermoplasty, however we also seek to expand the understanding of short duration heat effects at extreme temperatures and heat sensitivity of ASM, as little is known on these topics.

We first conducted a validation study of the model to demonstrate the internal temperature of the tissue after immersion in Krebs. Secondly, we conducted a study directly observing smooth muscle in tracheal strips; this also acted as a pilot to explore apoptosis detection methods *in situ*. Finally, we examined the effects of heating bronchial segments.

Specific Objectives

Validation Study

1. Confirm the internal temperature of tissue following immersion in heated Krebs buffer.

Tracheal Study (Pilot)

1. Examine the phenomenon of decreased functionality in smooth muscle following heating.
2. Determine whether cell death occurs following immersion in heated Krebs.
3. Determine whether cell death occurs through apoptotic mechanisms.
4. Determine the most appropriate methods for detection of cell death *in situ* and apoptosis following short duration exposure to extreme temperatures.

Bronchial Study

1. Examine the phenomenon of decreased functionality in tissues following heating.
2. Determine whether cell death occurs following immersion in heated Krebs.
3. Determine whether cell death occurs through apoptotic mechanisms.

Methods

Acquiring Tissue

Procedures were carried out on bovine lung tissue with approval from the Canadian Council on Animal Care guidelines and approved by the McMaster University Animal Care committee, the McMaster University Biosafety committee and the St. Joseph's Healthcare Research Ethics Board. Lungs and trachea were obtained at a local abattoir from euthanized cows (200-500 kg). Tissues were transported to the lab in ice cold Krebs buffer (NaCl, 116 mM; KCl, 4.2 mM; $CaCl_2$, 2.5 mM; NaH_2PO_4, 1.6 mM; $MgSO_4$, 1.2 mM; $NaHCO_3$, 22 mM; D-

glucose, 11 mM and indomethacin, 100 uM; bubbled with 95%O_2 / 5% CO_2 to maintain pH at 7.4) . Epithelium was removed from trachealis and strips (2 mm wide and approx. 10 mm long) of smooth muscle were excised while tissue was bathed in Krebs buffer. Lung was carefully cleaned of parenchyma, connective tissue and vasculature and bronchial segments (approx. 4 mm in diameter, 5 mm long) were excised while tissue was bathed in Krebs buffer. Bronchial segments were stored at 4°C and used in muscle baths within 5 hours of arrival to the lab.

Muscle Bath

Tracheal strips were mounted in the 4 ml muscle baths vertically using silk suture (Ethicon 4-O) and secured to a glass rod on one end to act as an anchor and to a Grass FT.03 force transducer on the other end. Bronchial rings were secured horizontally on small triangular wire mounts within the muscle baths and were attached with silk suture to the force transducer; these were also anchored to a glass rod. Muscle baths contained N-ϖ-nitro-L-arginine (L-NNA; 10^{-4} M) in Krebs buffer with indomethacin, kept at a temperature of 37°C and bubbled with 95% O_2/5% CO_2. Prior to stimulating each contraction, tissues were passively stretched to a preload tension of 1g. Isometric changes in tension were digitized (1 sample per 0.5 s) and recorded by DigiMed System Integrator software (MicroMed, Louisville, KY).

Prior to commencement of the experiment, tissues were equilibrated for 1 hour; following which, tissues were tested for functionality by challenging with 60 mM KCl three times. Experimental protocol began with a normothermic control response then washing of the drug. The tissue was allowed to relax prior to untying and immersion in Krebs buffer heated to the target temperature (37-95°C) for 30 s (trachea) or 1 min (bronchi). The tissues were then remounted in muscle baths and challenged with a second normothermic control response following 1 h or 24 h. To record the normothermic responses, tracheal tissues were challenged with Ach (10^{-5} M) and bronchial rings were challenged with KCl (60 mM). Tissues which remained for a 24 h period had gas reduced overnight and were covered with aluminum foil to promote survival of tissue.

Model Validation

A temperature probe was inserted into liquid silicone gel and left to solidify. Using a razor blade, gel was cut as a square to a diameter of 6 mm, sides equidistant from the probe centre. The embedded probe was then immersed in Krebs heated to 55°C for 1 minute with temperature measurements recorded every 2 s. The gel was cut to a diameter of 4 mm, 2 mm and <1 mm and the recording procedure was repeated at each distance.

A similar process was repeated using tracheal tissue. A sheet of bovine smooth muscle was dissected from a trachea and wrapped tightly around the probe using silk suture with a diameter of 4mm with the probe in the centre. The preparation was then immersed in heated Krebs buffer at a temperature of 55°C for 1 minute and recordings were taken at 2 s intervals. Recordings were visualized using Graphpad Prism v 5.0 to evaluate speed of heating.

Histochemistry

Following functional assessment, tissues (bronchial segments) were left for 30 min to relax or (tracheal strips) preloaded with 1g tension and relaxed with isoproterenol (10^{-6} M) and nitric oxide donor, S-nitrosylacetylpenicillamine (10^{-5} M), secured on wire scaffolds and placed in 10% buffered formalin. Tissue was fixed for 24-72 h and sent for processing at the Hamilton Regional Laboratory Medicine Program. Tissue was embedded in paraffin wax; tracheal sections to be sliced longitudinally and bronchi to be cut in transverse sections.

Paraffin embedded samples were rough cut and placed on ice for >1 h prior to slicing. Slices were cut using a microtome at 5µm for H&E staining, 3 µm for immunohistochemistry or 7µm for TUNEL staining. Slides were mounted on frosted slides (H&E), poly-L-lysine coated slides (trachea) or Superfrost Plus

slides (bronchi) in a water bath heated to ~40°C. Slides were left to air dry prior to staining.

Hematoxylin & Eosin

Tracheal tissues were sliced (5 µm thick) and mounted on frosted slides. They were then hydrated in three changes of xylene for 5 minutes each, three changes of 100% ethanol, one of 95% ethanol and one of 70% ethanol for 1 min each and running tap water for 5 min prior to immersion in Mayer's Hematoxylin for 10 min, 1 min TBS to blue, 4 dips in 1% acid alcohol and 5 min in Eosin. Tissues were then rinsed and dehydrated for 20 dips in 2 changes each of 70%, 95% and 100% ethanol and xylene and mounted using Permount.

Light microscopy was used to visualize tissue. Two independent assessors under blinded conditions examined the slides for gross morphological signs of cell death (condensed chromatin, apoptotic bodies, integrity of tissue, granularity/vascularization of cytosol, denucleation). Tissues were scored on a categorical scale (0, none; 1, mild; 2, moderate; 3, severe). The assessors were shown certain of the normothermic controls (which were defined as "0"), but were blinded with respect to the thermal treatment which the other samples received.

Immunohistochemistry

TUNEL

TUNEL was carried out using TACS Blue label kit (Trevigen Inc.). Tissues were sliced at 7 µm and mounted on poly-lysine coated slides. Slides were baked for 10 min at 57°C and left to cool for 10 min. Slides were hydrated in three changes of xylene for 5 minutes each, three changes of 100% ethanol, one of 95% ethanol and one of 70% ethanol for 1 min each and running tap water for 5 min. Slides were then circled with an immunopen and immobilized in 1x phosphate buffered saline (PBS). Samples were covered for 25 min at 37°C with proteinase K to retrieve antigen then covered in quenching solution (3% H_2O_2 in PBS) for 5 min. Slides were blocked using labeling buffer and covered with labeling solution for 1 h at 37°C in a humidity chamber. Labeling was stopped by covering the samples with stop buffer for 5 min. Slides were then covered with streptavidin horse radish peroxidise diluted in blue diluent solution for 10 min at 37°C before covering with blue label solution for 5 minutes. Slides were then counterstained with Nuclear Fast Red for 40 s and dehydrated for 10 dips in 2 changes each of 70%, 95% and 100% ethanol and xylene. Samples were mounted using Permount and left to dry.

TUNEL stains were visualized using Northern Exposure and three representative pictures were taken of each slide. The number of stained nuclei and total number of nuclei were counted by two observers under blinded conditions. Data was expressed as a fraction of labeled/total cells for analysis.

Alpha Smooth Muscle Actin

Alpha smooth muscle actin staining was completed on paraffin embedded bronchial tissues sliced to a thickness of 4 µm. Tissues were baked at 70°C for 20 min and hydrated in 3 changes of xylene, 3 changes of 100% ethanol, one 95% ethanol, one 70% and 5 min in running tap water. Slides were then placed in a preheated steamer with citrate buffer (0.1M) for 20 min for antigen retrieval. Slides were rinsed with distilled water, circled with an immunopen and immobilized in TRIS-buffered saline (TBS) for 5 min. Endogenous protein blocking was completed using 3% hydrogen peroxide in TBS for 5 min. Protein block (Dako, X0909) was added for 10 min followed by primary antibody (1:100; Dako, M0851 diluted in Dako, S3022) for 30 min. Yellow link secondary antibody and red link streptavidin peroxidise from Dako (K0690) followed addition of primary. AEC chromogen was added for 10 minutes to develop staining. Samples were counterstained in Mayer's Hematoxylin and mounted using Faramount

Aqueous Mounting Medium (Dako, S3025). Slides were visualized using Northern Exposure software.

Caspase 3

Caspase 3 staining was carried out on bronchial segments sliced to a thickness of 3 µm. The procedure occurred as explained above, using the same steps and reagents but replacing aSMA primary antibody with active caspase 3 antibody (cell signaling).

Immunofluorescence

Fluorescence staining was carried out on paraffin embedded tracheal tissues cut to a thickness of 6 µm. Hydration, antigen retrieval, blocking endogenous peptides and application of primary antibody followed the same steps outlined above for Caspase 3 and TUNEL staining. All later steps occurred in minimally lit conditions. The secondary antibodies and development were replaced by a fluorescent secondary antibody (Alexafluor red, TUNEL and Alexafluor green, Caspase-3). Slides were mounted using DAPI (UltraCruz).

Tissue was visualized using a fluorescence microscope and 3-5 corresponding and representative pictures were taken of each fluorescent tag,

depending on size of the tissue. Images were compiled using ImageJ software and observed for co-labeling within cells.

Results

Validation Study

Verification of Heat Penetration

Questions have been raised regarding the internal temperature of the tissues following 30 s immersion in the Krebs Solution. To answer these concerns, a thermometer was embeded within agarose gel of varying thickness and temperature measurements from the probe were recorded at 2 s intervals (fig. 2). This process was repeated with the thermometer encased in tracheal

smooth muscle tissue (fig. 3). The target temperature of 55°C was reached within 30 s when embeded in gel with a <2 mm diameter and in tracheal smooth muscle at a thickness of <4 mm. Experimental tissues were ~2 mm in diameter.

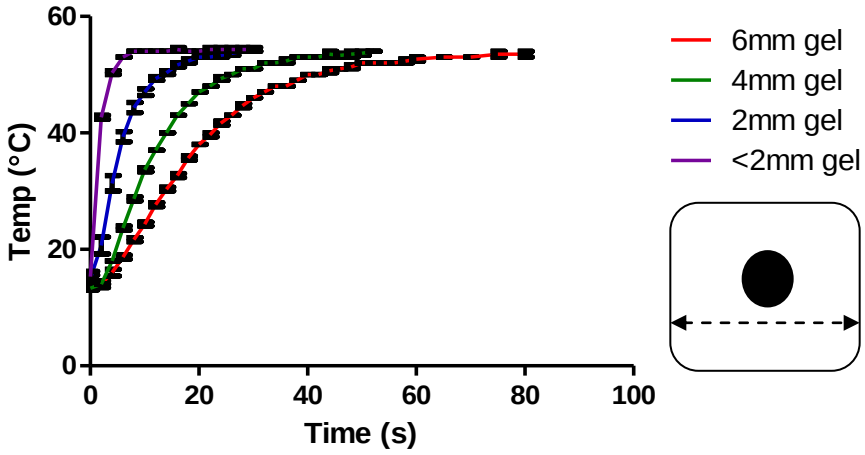

Figure 2. Recordings were taken at 2 second intervals of the temperature at the centre of aragose gel with a cross section of 6, 4, 2 and < 2 mm (n=3).

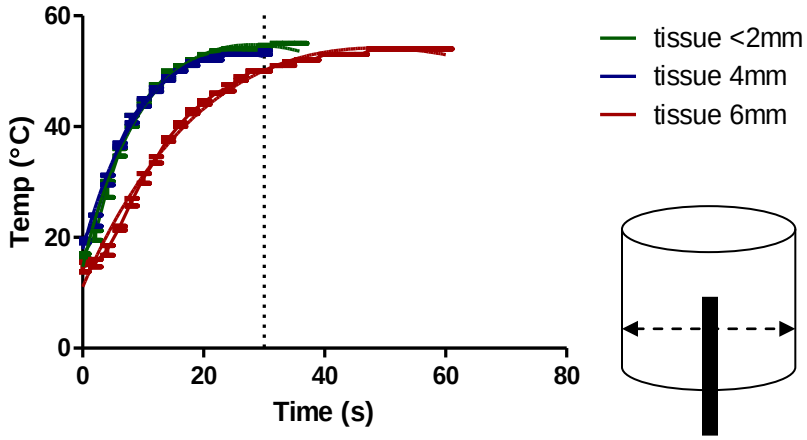

Figure 3. Recordings were taken at 2 s intervals of the temperature at the centre of tracheal smooth muscle tissue with a cross section of 6, 4, and < 2 mm (n=3). Tissues with a diameter of 4 mm reached the target temperature within 30 s.

Tracheal Study Results

Contractile Response is Reduced in Bovine Trachea Following Heating

Bovine tracheal tissues were hung in a muscle bath and were contracted using acetylcholine. Following heating, tissues were contracted a second time and normothermic contractions were compared. In tracheal tissues which were immersed in Krebs for 30 s the 37°C treated control tissues continued to show maximal response following heat application, 55°C treated tissues showed approximately 30% response whereas 65°C and 95°C treated tissues showed no response (fig. 4). This was evident after both 1 h and 24 h had elapsed. There was no obvious change in potency between 1 and 24 h.

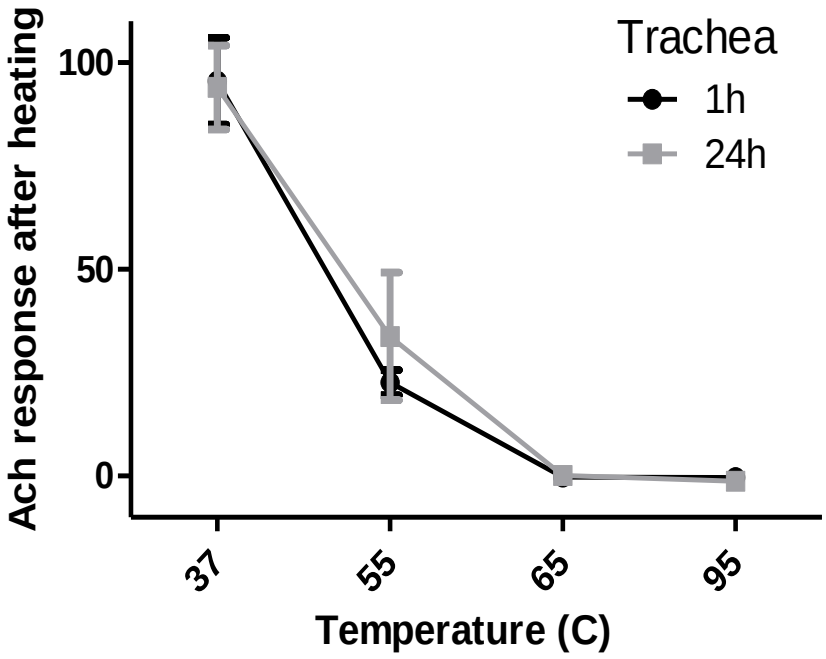

Figure 4. Graph depicting the force generation of bovine tracheal tissues following heat treatment. Response is recorded as percent of normothermic response preceding heat application. In the trachea, control tissues responded at maximal and 55°C treated tissues at 30% of maximal, whereas 65°C and 95°C tissues did not respond after heating (n=6).

Gross Morphological Damage does not Differ between Heated and Control Tissues

Twenty minutes after treatment, characteristics of cell death were visible which included a disrupted cytoplasm and disorganized nucleus (Fig. 5). The difference between treatments was not significant. Trends were observed in which absent to mild levels of cell death and moderate to severe levels of cell death in the 37°C and 95°C controls respectively; whereas, cells given treatment of 55°C and 65°C exhibited intermediate levels of cell death (Fig. 6). Following 24 h, similar trends are visible (Fig. 7); however, 55°C treated tissues exhibit cell death scores that are similar to those seen in 95°C ablative control tissue. Interestingly, following 24 h, tissues treated at 55°C maintain some functionality in the normothermic response and contraction could be observed to fluctuate when Krebs buffer was changed prior to normothermic challenge (data not shown).

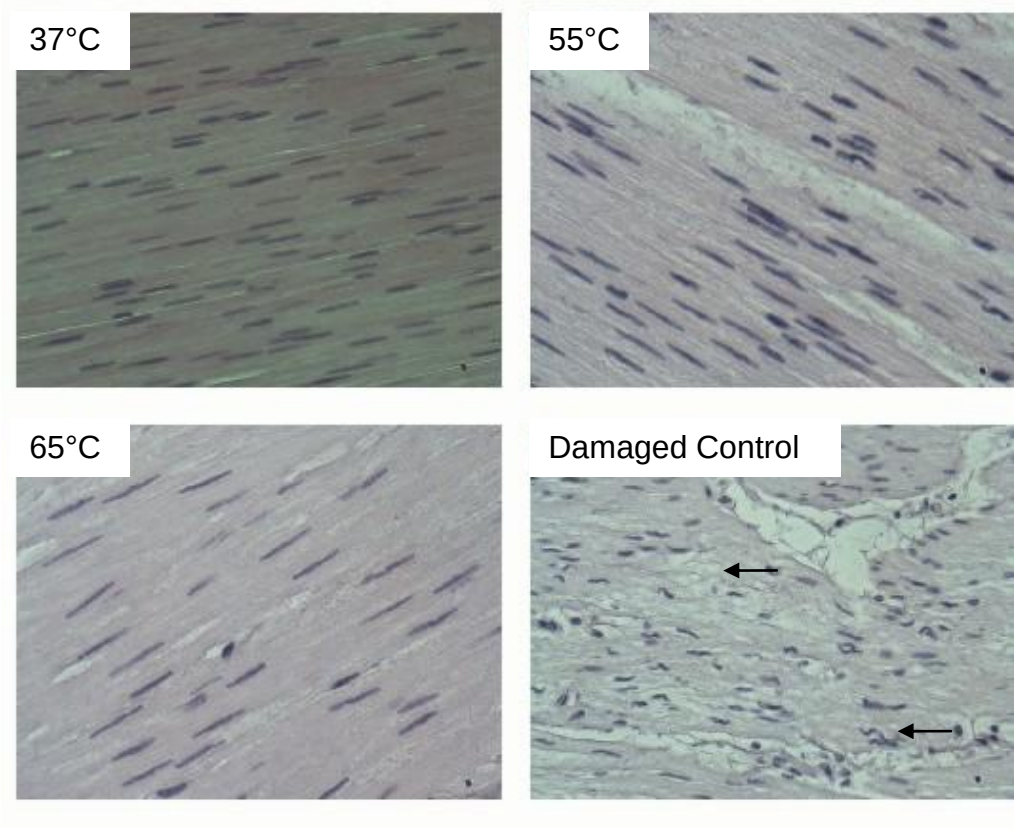

Figure 5. Images of smooth muscle cells following hematoxylin and eosin stain. Tissues treated for 30 s at 37°C, 55°C and 65°C exhibit minimal cytoplasmic and nuclear disruption. The damaged control is representative of tissue with gross morphological damage (disrupted cytoplasm, condensed nuclei, poor overall integrity of tissue, etc.)

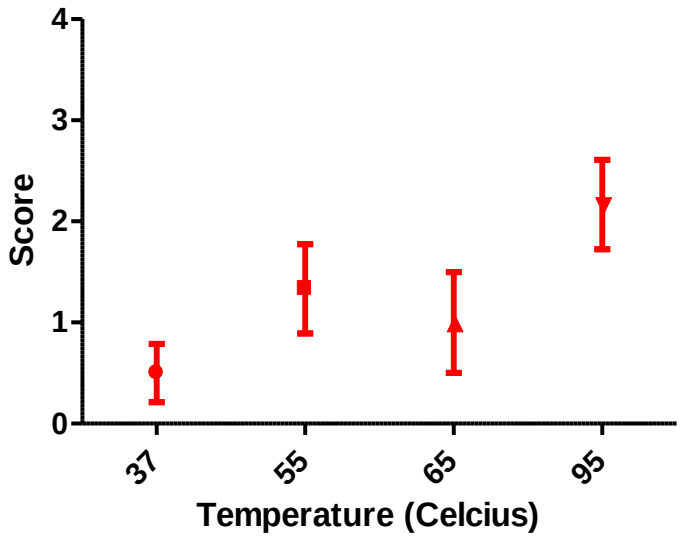

Figure 6. Cells given heat treatment of 37°C, 55°C, 65°C or 95°C were scored in a blind test by pathologists for the amount of cell death visible after 20 min. The difference is not significant (n=3, P=0.16).

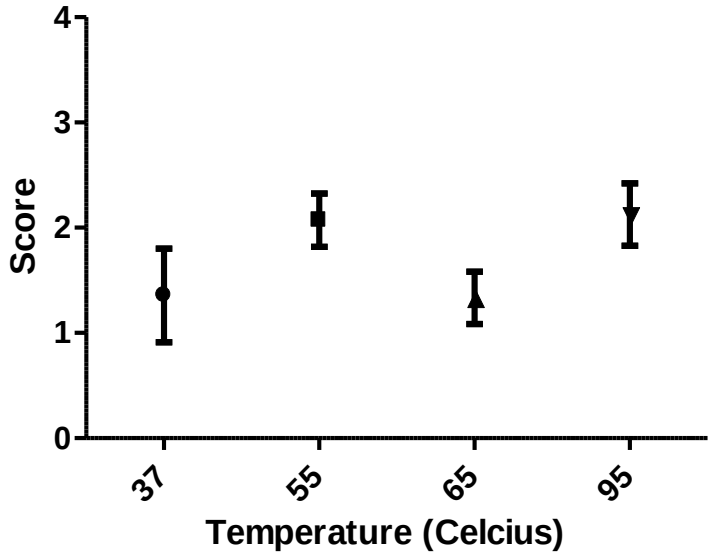

Figure 7. Cells given heat treatment of 37°C, 55°C, 65°C or 95°C were scored in a blind test by pathologists for the amount of cell death visible following 24 h. The difference is not significant (n=6, P=0.19).

Heat Treated tissues show increased levels of DNA Cleavage in situ

Tissues fixed 1 h and 24 h after treatment were stained using TUNEL. Stained cells indicate DNA cleavage has occurred, exposing 3' hydroxyl ends of DNA; this is a characteristic of apoptotic cell death and necrotic cells may also exhibit this staining as they have undergone non-specific cleavage [95]. Blue nuclei indicate TUNEL labeling as visible in nuclease treated cells which acts to artificially cleave DNA during the staining process and act as a control (Fig. 8a). A control, 37°C tissue serves as a comparison for heat-treated cells (Fig. 8b) and treatments of 55°C and 65°C were applied (Fig. 8c,d). Stained cells were quantified and expressed as a fraction of total cells. A significant difference between control and treated tissues of 55°C and 65°C is noted 1 h following heating (Fig. 9). A significant difference between control tissues and 65°C treated tissues is noted 24 h following application of heat (Fig. 9).

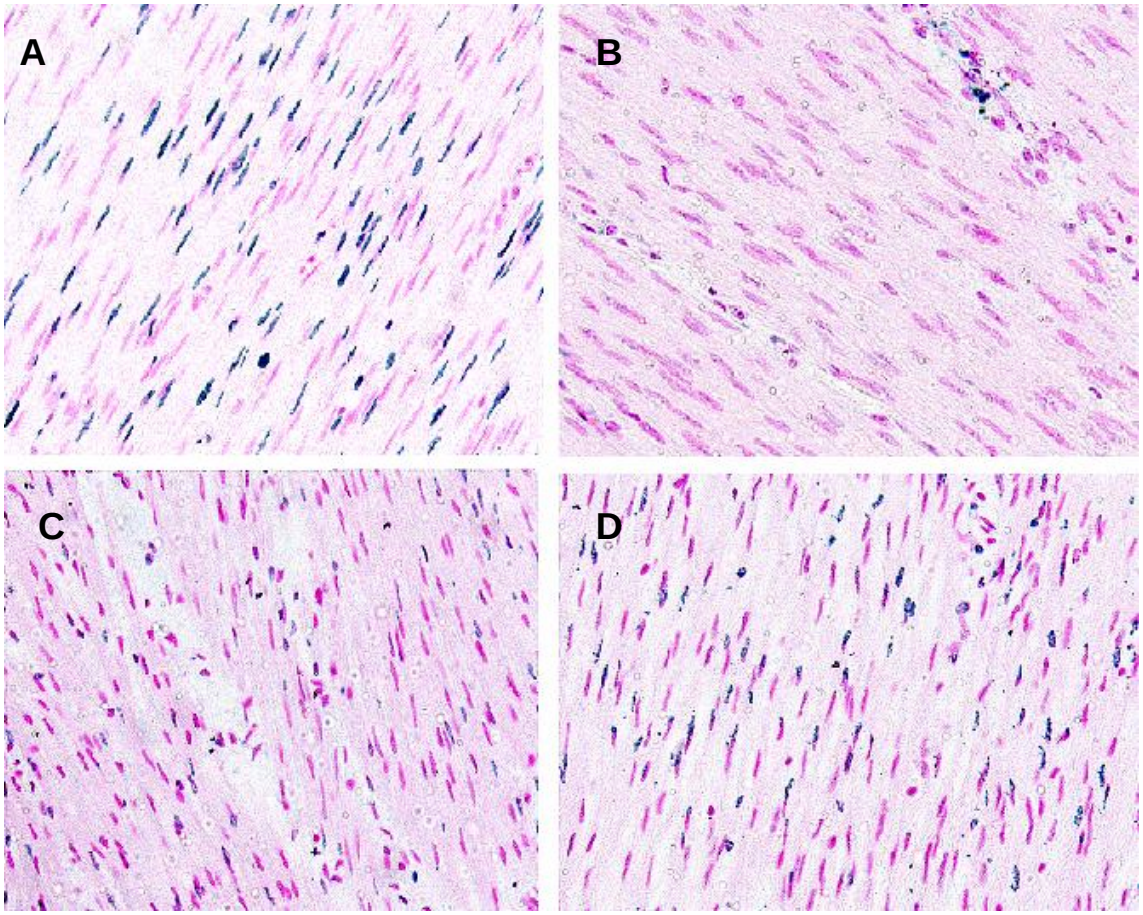

Figure 8. Images of smooth muscle cells following a TUNEL stain. A control stain that has undergone artificial apoptotic cleavage by TACS-Nuclease™ (A) as well as tissues treated for 30 s at 37°C (B) 55°C (C) and 65°C (D) are shown.

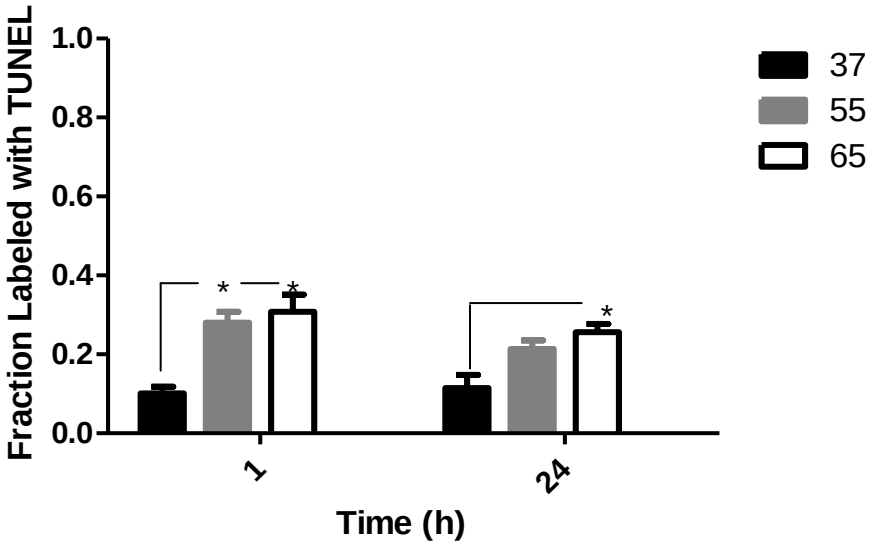

Figure 9. TUNEL stain data expressed as fraction of stained cells 1 and ~24 h after heat treatment. There is a trend suggesting increasing cell death of the 55°C and 65°C temperatures at the 24 h time point. (Kruskal Wallis; $P<0.05$, $n=3$).

TUNEL co-localizes with Caspase 3 in 55°C, not 65°C treated tissue

The appearance of active caspase 3 and DNA cleavage, as indicated by TUNEL staining, localized to the same cell would indicate that cells have undergone or are undergoing apoptosis. Control tissue treated at 37°C is able to undergo this process and exhibit co-localization of green (caspase 3) and red (TUNEL) at 24 h (Fig. 10a). Tissues treated to 55°C also exhibit some co-localization of these labels (Fig. 10b). However 65°C treated tissue do not exhibit co-localization of these two signals (n=2, 3; 1 h, 24 h).

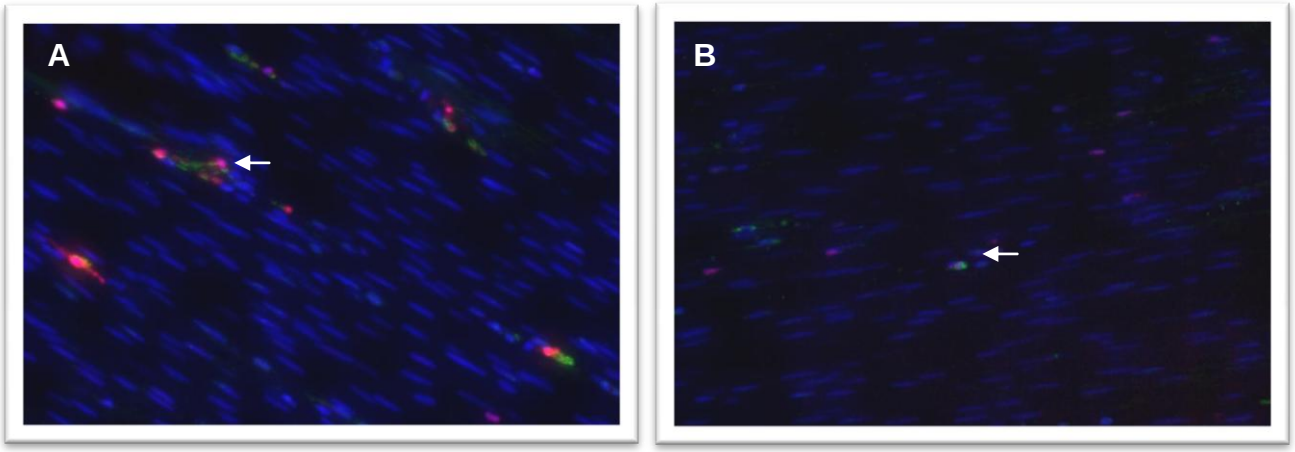

Figure 10. Images of smooth muscle cells following a fluorescent caspase-3, green, and TUNEL, red, double stain. (A) A 37°C control at 24 h that has some apoptosis evident (co-localization of caspase 3 and TUNEL) is depicted along with (B) a 55°C control slide in which some apoptosis is evident. Small amounts of apoptosis were evident in 55°C treated slides while none were visible in 65°C slides.

Bronchial Study

Contractile Response is Reduced in Bronchi Following Heating

Bovine bronchial tissues were hung in a muscle bath and were contracted using a dose of potassium chloride that would produce maximal contractility. Following heating, tissues were contracted a second time and normothermic contractions were compared (Fig. 11). Bovine bronchial segments were heated for 1 minute to ensure uniform heating of the smooth muscle layer. At 1 h, 37°C control tissue was able to exert a near maximal response, 52°C demonstrated a half maximal response and 55°C and 65°C treated tissues showed little to no response. Following 24 hours, control tissues had decreased to half maximal response, 52°C tissues had retained a half maximal response and 55°C and 65°C treated tissues still showed little to no response.

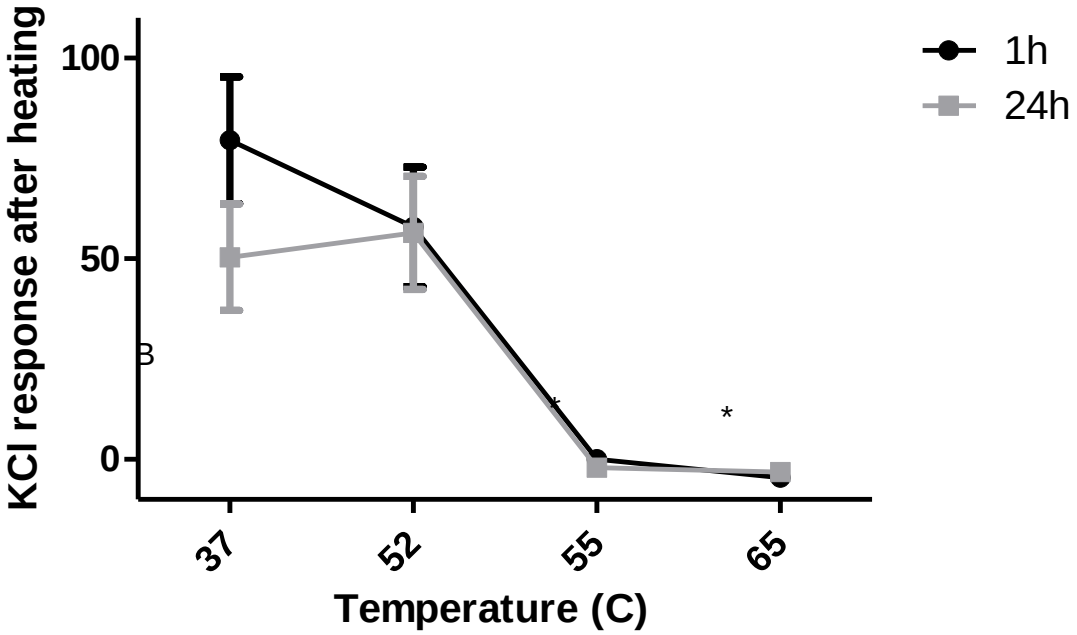

Figure 11. Graph depicting the force generation of bovine bronchial tissues following heat treatment. Response is recorded as percent of normothermic response preceding heat application. In the bronchi, control tissues responded almost maximally after 1 hour and 50% of maximum following 24 h, 52°C tissues responded at half maximum 1 and 24 h following heat treatment and 55°C and 65°C tissues did not respond at both 1 and 24 h (n=4). * indicates significant difference from 37°C and 52°C tissues.

DNA cleavage is observed in 65°C treated tissue over time

Bovine bronchi were heat treated and fixed 1 h or 24 h after heat treatment. After which they were stained with TUNEL to detect DNA cleavage, a characteristic of apoptotic and some necrotic cells. All tissue exhibited some staining and after 24 h tissues treated with 65°C heat had significantly more stained nuclei compared to all other temperatures at 24 h and compared to 65°C treated tissues at 1 h (Fig. 12). The staining pattern in these tissues was also different than that seen in tissues at other temperatures (Fig. 13); staining was confined to the nuclei in most tissues, but in the 65°C treated tissues at 24 h, the staining also pervades the cytoplasm of counted cells. Furthermore, surrounding tissue appears to have gross morphological damage and epithelial cells are generally not intact.

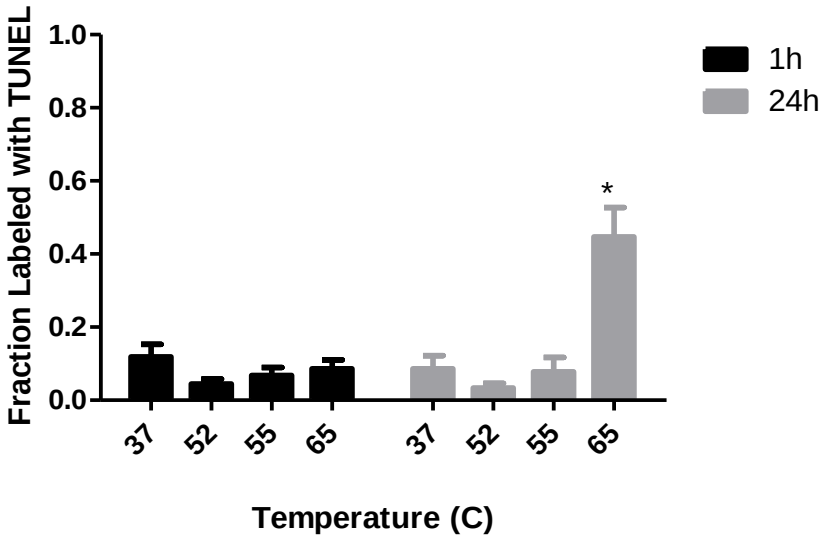

Figure 12. TUNEL stain data expressed as fraction of stained cells 1 and 24 h after heat treatment. There is a significant difference between cell death at 24 h in 65°C tissues compared to 65°C at 1h ($P<0.05$, $n=6$) and to other temperatures at the 24 h time point. (Kruskal Wallis; $P<0.05$, $n(37,52)=5$, $n(55,65)=6$).

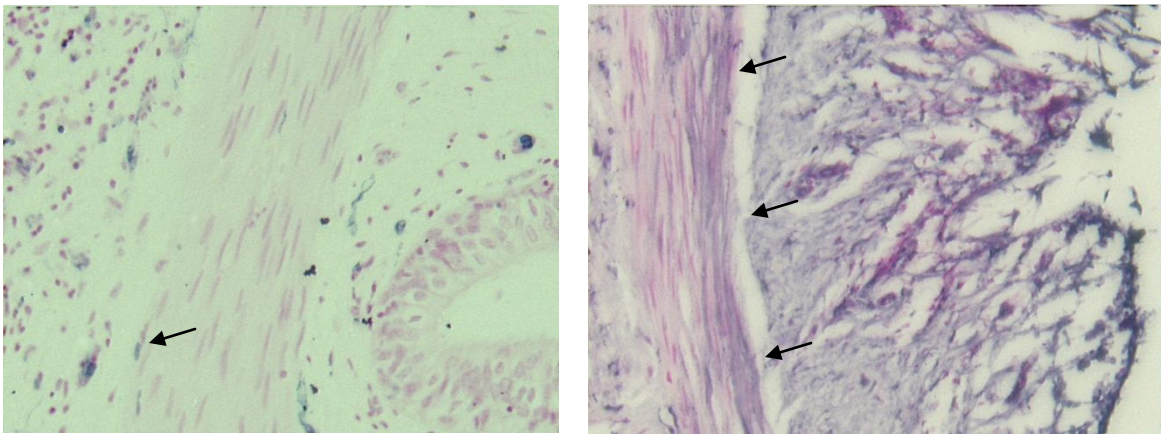

Figure 13. Images from the bovine bronchi TUNEL stain at 24 h. Compared to control tissue (A), positive staining has a different pattern in 65°C treated tissues, damage to the epithelium is also evident (B).

Cleaved Caspase 3 expression is effected by temperature treatment

Staining for cleaved caspase 3 was carried out on bovine bronchi at 1 and 24 h (Fig. 14) and results were quantified (Fig. 15). Variable amounts of caspase 3 staining were detected at all temperatures and time points. A significant effect of temperature was noted using a 2 way ANOVA ($F(3,39)=3.15$; $P=0.036$). No significant difference was indicated between data sets; however, Bartlett's test found a significant difference between variances (1h, $P<0.0001$; 24h $P=0.006$).

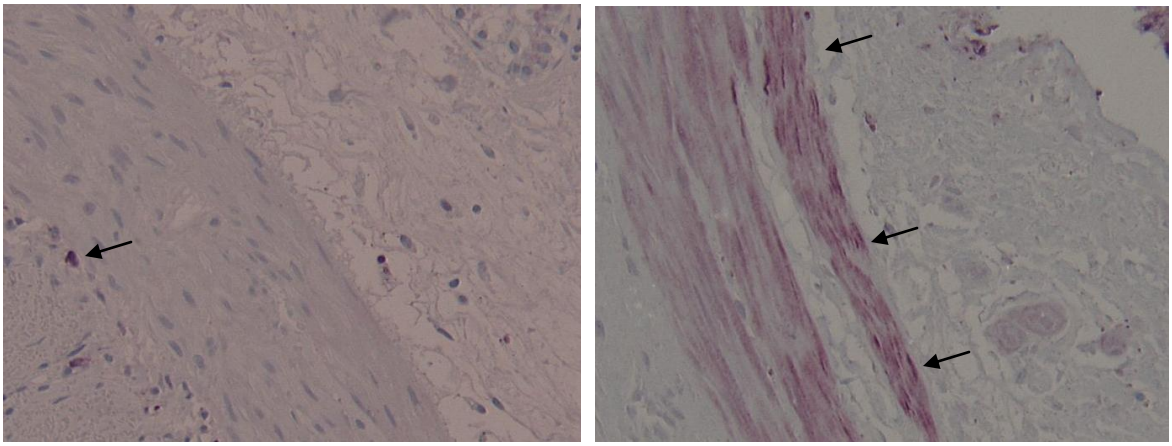

Figure 14. Images of cleaved caspase 3 24 h after heat treatment. (A) the majority of tissues had a similar appearance, showing limited amounts of apoptosis confined to specific cells. (B) tissues with >30% staining exibited a pattern with greater cytoplasmic staining, these were found in some tissues following 37°C and 65°C heat treatments.

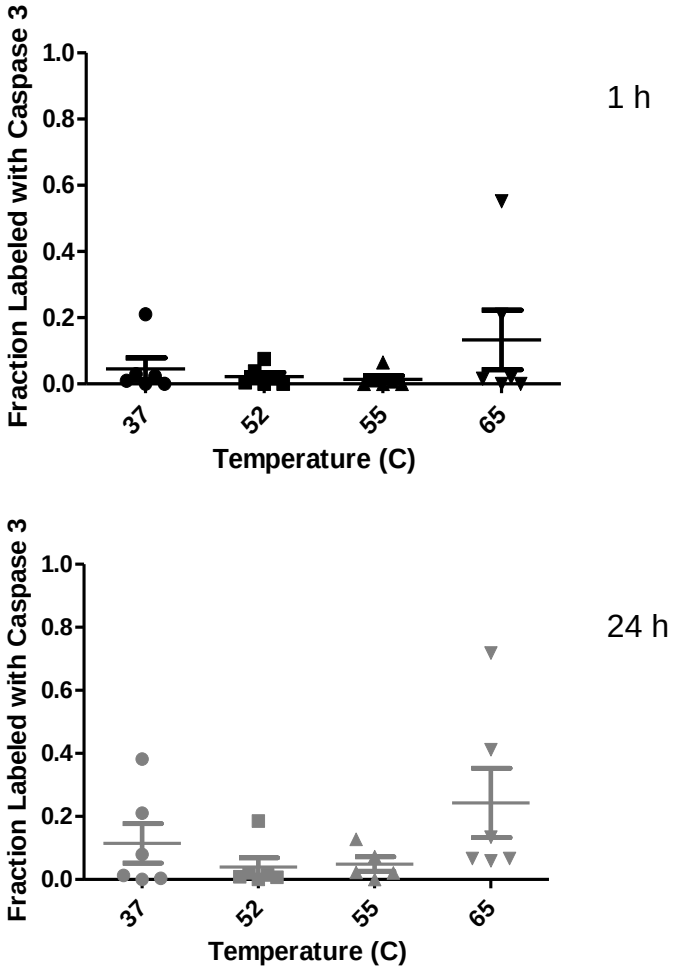

Figure 15. Cleaved Caspase 3 was quantified and expressed as a fraction of stained cells 1 and 24 h after heat treatment. There was a significant effect of temperature on stained cells ($F(3,39)=3.15$; $P=0.036$). No significance of time or time and temp interaction was indicated. There was also no difference between data sets, Bartlett's test for equal variance found a significant difference (1h, $P<0.0001$; 24h $P=0.006$).

Discussion

Overall Findings

Bronchial thermoplasty is thought to act through targeting of the ASM tissue to reduce smooth muscle mass; however it is currently unknown what cellular events underlie the loss of ASM following heating seen in preliminary investigations on dogs and humans. Here, experiments have been conducted on *ex vivo* heated bronchial segments to note the effects on functionality and markers of cell death.

To examine smooth muscle effects, a model was utilized in which tissue was immersed in heated Krebs buffer. We first validated the model by demonstrating that the heat penetration following immersion was able to reach target temperatures within 30 s. We also incorporated functional assessments in muscle baths which verified previously published ablative effects on contraction in trachea and bronchi [62]. Finally, we noted effects on cell death markers of morphology, DNA cleavage and caspase activation. These experiments were first carried out on tracheal smooth muscle strips and repeated on bronchi with optimized *in situ* cell death detection methods.

We have noted that when heated to 65°C tissues experience increased DNA cleavage and some caspase 3 expression. This demonstrates that bronchial segments treated for 1 minute with 65°C heat are undergoing cell death within 24 h. At this temperature, and also at 55°C, contractile mechanisms within the tissue do not function. When heated for 1 minute at lower temperatures of 55°C, 52°C or 37°C tissues do not experience increased DNA cleavage and they have low levels of active caspase 3. The 37°C and 52°C tissues maintain functionality. This suggests that cell death involving cleavage of DNA occurs between 55°C and 65°C and that functionality in these tissues ceases at temperatures between 52°C and 55°C when heated for short durations.

Model Translation

This study represents the second use of this heat immersion model to demonstrate the effects of extreme temperature on ASM. Here we have shown that the temperature penetration does reach the centre of heated tissues using a thermometer embedded in agarose gel and also within tracheal ASM *per se*. The model is able to demonstrate temperature effects and the model validation experiment suggests it is suitable for further investigation into the cellular effects of short duration heating at extreme temperatures.

This model uses thermal energy to effectively demonstrate the effect of target temperatures on smooth muscle tissue; it cannot directly observe the effects of 10 s exposure to RF due to the different heating method. RF energy will penetrate deeper into tissues immediately so time requirements of thermal conduction may interact differently when approaching key temperatures.

With this approach, we have observed effects on smooth muscle using animal tissue. Human ASM is similar to other species in structure and mechanics [99]. While properties of ASM are conserved across species, it would be possible to replicate measurements using this model in human tissue or airways. The thermal model is also beneficial as we are able to isolate smooth muscle tissues from other physiological inputs and understand specifically temperature effects on ASM.

Tracheal Pilot vs. Bronchial Results

Importantly, the approach of the heat application varied between the pilot tracheal study and the bronchial study. The tracheal tissue was dissected as strips of ASM, whereas the bronchial segments contained epithelium, cartilage, ECM and in some cases parenchyma. These models were selected to first note the effects of heat directly on smooth muscle using a straightforward tracheal strip model and then to observe tissue *in situ* using the bronchi, which is also more relevant to bronchial thermoplasty as a model. Treatment time was extended in the bronchial model to ensure penetration of heat to the smooth muscle layer of the airway segment. Having said this, we expect the temperature of the tissue would be similar (see *Model Translation*).

At 55°C, tissues were entirely unable to contract in bronchial segments but there was still a half maximal contraction in trachea. In the paper by Dyrda and colleagues[62], a similar trend was noted whereby the complete ablation of function occurred at 55°C. Their experiments regarding duration of heat exposure showed no evidence of a significant difference based on the time-course; however following 1 min of heating in tracheal strips, function ceased in 55°C treated tissues and after 20 s at the same temperature, tissues still showed some response. Other studies have also noted a difference in cell response based on heating duration [34,100]. The duration of heating effect is also supported by shifts in

phase transitions when varying speed of heating in differential scanning calorimetry studies [101]. This time course effect may be due to the energy input to the tissues, in addition to the absolute temperature.

Contractile vs. Vitality Response to Heat

Contractile function does not depend on the vitality of a cell, nor must a smooth muscle cell require a functional contractile apparatus to be alive. This is evident from studies which isolate contractile proteins and stimulate their function (motility assays for example [62,102]) and from experiments which compromise cell survival by making the membrane permeable and can still exhibit measurable contractile responses [103]. Furthermore, smooth muscle cells are readily cultured and these cells are viable but in a non-contractile phenotype, as are smooth muscle cells in various stages of the cell cycle.

There is a similarity of the contractile and vital processes in these experiments which demonstrates dysfunction at comparable temperatures. This must be considered a correlation and not causative until proven otherwise. The thermal profile of nuclear matrix which denatures at ~51°C [87] is similar to that of myosin which denatures at ~52°C[89]; these proteins are key players in cell viability and cell contractility, respectively. Influence of the contractile mechanism may

have an indirect influence on survival because of dual role of HSP27 (See *Apoptotic Effect*).

Control tissues

Included in this study were control tissues that had been immersed in Kerbs buffer heated to 37°C. These were used as control tissues for the functionality assessment as well as the apoptotic staining assessments. While conducting these experiments, particularly in the bronchial 24 h experiments there were some issues with survival of the tissues and continued contractility.

In the functional assessment of the bovine bronchi, 37°C treated tissues were the only set to experience a declining trend in functionality over time and in the tracheal fluorescence stain co-labeling of cells was visible. Furthermore, H&E stains of tracheal tissue, cleaved caspase 3 and TUNEL staining of both tissues was observed to be above the baseline. Serum starvation is used as a control in apoptosis experiments [77,104] and this condition may be promoting apoptosis in our experimental tissues over time, which would also be exacerbated by any injury caused during handling. It is important to note this when interpreting data from the study. Simply put, 37°C should not be considered a baseline tissue with no cell death present, and should in fact be viewed as a positive control demonstrating some apoptosis.

Our maximal temperature used in the bronchial studies was 65°C. We chose to include an intermediate temperature that reduced contractile function by approximately 50%, 52°C, rather than the 95°C temperature used in the tracheal studies. In the tracheal studies a similar response from the 65°C and 95°C in contractile experiments and the H&E staining is observed. However it cannot be concluded from these data that the 95°C temperature causes more cell death than the 65°C treatment. In other studies, scalding occurs over 95°C due to evaporation from tissues[71] and several proteins including actin and DNA undergo thermal transitions between 70°C and 95°C[63,88,105].

Cell Death Detection

Cell death detection often centers on three general characteristics: DNA cleavage, morphological/membrane changes or caspase activation. In cell culture, assays are readily available which may observe these characteristics [94]. However in intact tissue slices, many of these detection methods are not applicable and the primary tool for observation is immunohistochemistry. The methods selected in this study represent these three categories of cell death observation – DNA cleavage, tissue morphology and protein activation.

We found gross tissue morphology based on H&E staining and scoring to be a weak method to observe cell death in smooth muscle following short

duration heat treatment. Differences were not noted between heat treatments or control tissues, and moderate evidence of cell death was visible at all temperatures. This model was not robust in discriminating dead tissue. Quantification of TUNEL proved to be a more discerning assessment of cell death *in situ*. In both tracheal and bronchial tissues, significance discerning temperature effect on cell death was achieved.

Fluorescence co-localization was also attempted in tracheal tissues. This enabled us to say conclusively that apoptosis was able to occur; however we were unable to quantify this trend. Thus, we opted to use a histological caspase stain and quantified the number of cells visible to investigate the bronchial response. This approach was able to reduce subjectivity and compare amounts of protein activity.

Through the methods of detection, we run into questions around the defining characteristics of cell death. Here we observed that at temperatures of 55°C the DNA is not cleaved and the caspase 3 is minimally expressed; this would normally indicate viability of the tissue. However, this tissue is not able to contract and the critical temperature for cell viability hovers around the nuclear matrix transition temperature (48-55°C) [87].

The process whereby cells have ceased to be functional due to the denaturation of proteins is called coagulation necrosis. In this state a cell is unable to undergo apoptosis because of the accumulation of insoluble

aggregates. Due to the nature of the heat treatment it is reasonable to question whether the cell is metabolically active despite the evidence which does not conclude that cell death has occurred.

Apoptotic Effect

When approaching higher temperatures in long term heating of cells in culture it has been reproducibly established that there is a progression from apoptotic to necrotic cell death [65,74,84,96]. This change has been observed to occur at hyperthermic temperatures with variation depending on cell priming, cell type or duration of heating [83]. We have noted an effect of temperature on cleaved caspase 3 expression indicating apoptosis may be occurring in some tissues at certain temperatures. The minimal TUNEL staining at temperatures below 55°C and minimal expression of caspase 3 suggests that ASM treated below this temperature may not be dying. Alternatively, denaturation of proteins may inhibit metabolic activity or the presentation of cell death markers.

This departure from cell death temperature parameters noted elsewhere [34] may be attributed to the difference in duration as well as the influence of HSP27 and other chaperones present in ASM. Duration of heating will impact the amount of energy input into the cellular system (See *Temperature Effects – Temperature Profiles*)

Small heat shock proteins are involved with actin stabilization in the contractile mechanism, and are likely present in higher concentrations in smooth muscle tissue where they hold this dual role. Small heat shock proteins are able to renature following the heating [75] and may then act as chaperones that sequester unfolded proteins to allow normal functioning of the cell by blocking apoptotic effects[32,106]. Intermediate stages such as 52 and 55°C do not have enough damage to alter TUNEL by causing damage to DNA, but would be sufficient to denature myosin and may affect other key signaling proteins essential to the apoptotic cascade. This would prevent apoptosis to the extent it is observed in 37°C either because proteins involved in the cascade are unable to perpetuate the process or because small heat shock proteins would confer thermal resistance to injured cells[36].

Heat tolerance related to the upregulation of heat shock proteins has been noted in tissues heated for more than 15 min to a sub-lethal temperature, ~43°C [107]; this may be similar to the protective effect noted at 52°C and 55°C. It could be that upregulation of chaperones would prevent death due to serum deprivation or hypoxia as occurs in control tissues. HSP27 shows maximal upregulation following 1 minute of 50°C heating and is still expressed up to 56°C [34].

Zones of coagulation correspond to areas that have reached a minimum of 65°C following tumor ablation[68,93]. This type of necrosis does not show classical signs of apoptotic cell death (cleaved caspase 3), morphology does not differ

(histology) and protein unfolding or dysfunction is evident (myosin motility assay). Based on the evidence gathered here showing cleaved caspase 3 expression in some tissue slices, cell death occurring at 65°C in the ASM of bronchial segments may include some apoptosis as well. Experiments show consistently high levels of TUNEL and variable levels of cleaved caspase 3; particularly, those with high cleaved caspase 3 levels may indicate an apoptotic response was initiated within the tissue.

Effect of Heat on Smooth Muscle Tissue

One major purpose of this study was to build on knowledge about the effects of extreme temperatures on ASM. What we currently know comes from a paper by Dyrda *et al* [62]. They were able to demonstrate the functional consequences, including functional cessation at 65°C in trachea and 55°C in bronchi, which we have reproduced here. They also demonstrated that the myosin protein which is fundamental to contraction is not functional but the actin maintains functionality.

We further investigated the short term effects of thermoplasty by confirming their functional measures and investigating cell death effects. Cell death effects do not directly relate to the functional effects, except based on the correlation of denatured proteins which are implicated in both outcomes (see

functional vs. vital effects). What we do note is that tracheal and bronchial tissues treated to a target temperature of 65°C will undergo a process of cell death and that cleavage of DNA will occur within the first 24 h. We further observe that classical signs which indicate apoptosis and necrosis are not substantially visible in tissues treated to target temperatures of 55°C or less.

Bronchial Thermoplasty Procedure

The bronchial thermoplasty procedure is performed over three visits lasting approximately 1 hour each. Possible alterations in the procedure are under investigation to reduce the time required to complete the treatment. For example, a model was created based on a six arm basket which is moved every three seconds as opposed to the current 4 arm system that is transposed every 10 seconds [51]. If the same results can be produced, it would reduce procedural time requirements by a third.

Adjustments to the frequency or wattage generated may have similar improvements on the delivery of this treatment. However, an alteration in the frequency would change the initial depth of energy penetration [69,71] making it even more vital to know the key target and effects of temperature on the tissue.

Thermoplasty has also been noted to have some early adverse effects on patients. However, few studies have been published that examine early events

following extreme heat exposure in smooth muscle. This period is clearly important to the health of individuals undergoing bronchial thermoplasty. By understanding molecular mechanisms of cell death that appear during this time we may be better equipped to stem adverse events such as these or any that may come up as the procedure becomes more prevalent. For example, the immune clearance of apoptotic and necrotic cells can produce an inflammatory reaction and processes such as liquefaction necrosis of leukocytes may produce pus and contribute to any mucus plugs observed.

Possible mechanisms of Bronchial Thermoplasty effect

There is still much controversy surrounding the bronchial thermoplasty treatment[49,50]. Many of the questions that remain involve the mechanisms behind bronchial thermoplasty; it is unclear at this time what the cellular mechanisms are behind the asthma quality of life effects.

Our study indicates cell death of ASM due to heating may reasonably be behind reduced smooth muscle mass that was noted in dogs and is suggested as a mechanism of effect in humans [48]. We found that tissues heated to 65°C, the target temperature of the bronchial thermoplasty procedure, will cause death in heat treated smooth muscle within the first 24 h. However, there are other

changes resulting from bronchial thermoplasty which may prove beneficial in combination with smooth muscle cell death.

Among suggested mechanisms are changes in the epithelial barrier, namely a decreased composition of mucus producing cells following repair and improved barrier function. As well, altered ECM composition may influence function of any surviving ASM and increase elasticity. Or, the removal of immediate immune influences relating to asthma may allow the immune process to “reset” avoiding overreactive processes in subsequent exposures. And effects which increase or normalize the airway diameter due to the procedure may also have positive breathing effects.

Potentially harmful effects may also be responsible for the benefits of bronchial thermoplasty. It has been suggested for example that nerves within the airways become fried, which would remove discomfort of the asthma attacks but leave the asthmatic airway phenotype without surveillance. Another potential hazard would involve the response to heat of excess inflammatory cells in the airways. In a process related to coagulation necrosis, necrotic leukocytes may release lysozymes and undergo liquefactive necrosis; thus, creating pus, worsening mucus plugs and contributing to early adverse effects. If this is the case reducing inflammation in the airways would be essential to limiting these effects. More information is needed to understand the positive effects of this procedure.

Further Work

In this study we were able to build on knowledge of the early effects of heat on smooth muscle as a model of bronchial thermoplasty. To further this work and follow up on other potential mechanisms of bronchial thermoplasty we will need to use in vivo models and lung biopsies.

Animal models have the advantage of having the physiological inputs such as nutrition and immune reaction that help to make knowledge transferable to humans and also allowing greater latitude of study compared to human subjects. Through the use of these models we will be able to note cell death that is occurring and also observe the immune reaction that results from heat application. Redness and edema have been noted previously [55] but the specific involvement of leukocytes in repair following the procedure has not been elucidated. As well, adverse effects increase in humans soon after treatment, so increased knowledge of physiological reactions to this treatment is vital to improve post-procedural care. Without nutritional input we noted substantial cell death in 37°C heated tissues (see *Control Tissues*). With physiological input and less handling of tissues, cell death due to starvation, hypoxia or damage should decrease and enable quantification of cells undergoing apoptosis and necrosis due specifically to the application of heat.

Lung biopsies have the advantage of being able to note differences in asthmatic airways before and after treatment. This will be particularly advantageous to note any differences in cellular compositions of the airways and making comparisons related to asthma. Suggested effects of bronchial thermoplasty include alterations in ECM composition, effects on innervations of the tissue or goblet cell concentration in the epithelium. This could be studied in a before/after model using lung biopsies. Collagen and elastin staining are common techniques as is staining for goblet cells; nerve cells can also be visualized in histological staining. Post thermoplasty sections could be stained for these targets and compared to the same individuals prior to treatment and to known cellular compositions in asthmatic vs. normal airways to see if there is an improvement.

Summary

A novel asthma treatment, bronchial thermoplasty, has shown improvements in AQLQ and has lasting positive effects on patients suffering with severe asthma. This procedure is suggested to act through extreme heat-mediated ablation of ASM. Here, we investigated the effects of extreme heat on ASM using a thermal model of bovine tissue immersed in heated medium. Functional cessation was confirmed and cell death was noted within the 24 h when treated for clinically relevant time periods at 65°C. As such, heat-mediated ablation of ASM is a plausible mechanism for the benefits observed following bronchial thermoplasty.

References

1. Statistics Canada. Asthma, by sex, provinces and territories. http://www40.statcan.ca/l01/cst01/health50a-eng.htm. Updated 2009.

2. Chetta A, Foresi A, Del Donno M, Bertorelli G, Pesci A, Olivieri D. Airways remodeling is a distinctive feature of asthma and is related to severity of disease. *Chest*. 1997;111(4):852-857.

3. Ellis R, Leigh R, Southam D, O'Byrne PM, Inman MD. Morphometric analysis of mouse airways after chronic allergen challenge. *Lab Invest*. 2003;83(9):1285-1291.

4. Chinellato I, Piazza M, Sandri M, et al. Serum vitamin D levels and exercise-induced bronchoconstriction in children with asthma. *Eur Respir J*. 2011;37(6):1366-1370. doi: 10.1183/09031936.00044710.

5. de Diego Damia A, Leon Fabregas M, Perpina Tordera M, Compte Torrero L. Effects of air pollution and weather conditions on asthma exacerbation. *Respiration*. 1999;66(1):52-58.

6. Lougheed MD, Lemiere C, Dell SD, et al. Canadian thoracic society asthma management continuum--2010 consensus summary for children six years of age and over, and adults. *Can Respir J*. 2010;17(1):15-24.

7. Crapo RO, Casaburi R, Coates AL, et al. Guidelines for methacholine and exercise challenge testing-1999. this official statement of the american thoracic society was adopted by the ATS board of directors, july 1999. *Am J Respir Crit Care Med*. 2000;161(1):309-329.

8. Lemiere C, Bai T, Balter M, et al. Adult asthma consensus guidelines update 2003. *Can Respir J*. 2004;11 Suppl A:9A-18A.

9. Juniper EF, Guyatt GH, Epstein RS, Ferrie PJ, Jaeschke R, Hiller TK. Evaluation of impairment of health related quality of life in asthma: Development of a questionnaire for use in clinical trials. *Thorax*. 1992;47(2):76-83.

10. Juniper EF, Buist AS, Cox FM, Ferrie PJ, King DR. Validation of a standardized version of the asthma quality of life questionnaire. *Chest*. 1999;115(5):1265-1270.

11. Kurashima K, Kanauchi T, Hoshi T, et al. Effect of early versus late intervention with inhaled corticosteroids on airway wall thickness in patients with asthma. *Respirology*. 2008;13(7):1008-1013. doi: 10.1111/j.1440-1843.2008.01384.x.

12. Leigh R, Ellis R, Wattie J, et al. Dysfunction and remodeling of the mouse airway persist after resolution of acute allergen-induced airway inflammation. *Am J Respir Cell Mol Biol*. 2002;27(5):526-535.

13. Bentley JK, Deng H, Linn MJ, et al. Airway smooth muscle hyperplasia and hypertrophy correlate with glycogen synthase kinase-3(beta) phosphorylation in a mouse model of asthma. *Am J Physiol Lung Cell Mol Physiol*. 2009;296(2):L176-84. doi: 10.1152/ajplung.90376.2008.

14. Carroll N, Elliot J, Morton A, James A. The structure of large and small airways in nonfatal and fatal asthma. *Am Rev Respir Dis*. 1993;147(2):405-410.

15. Aysola RS, Hoffman EA, Gierada D, et al. Airway remodeling measured by multidetector CT is increased in severe asthma and correlates with pathology. *Chest*. 2008;134(6):1183-1191. doi: 10.1378/chest.07-2779.

16. Shiba K, Kasahara K, Nakajima H, Adachi M. Structural changes of the airway wall impair respiratory function, even in mild asthma. *Chest*. 2002;122(5):1622-1626.

17. Mitzner W. Airway smooth muscle: The appendix of the lung. *Am J Respir Crit Care Med*. 2004;169(7):787-790. doi: 10.1164/rccm.200312-1636PP.

18. An SS, Bai TR, Bates JH, et al. Airway smooth muscle dynamics: A common pathway of airway obstruction in asthma. *Eur Respir J*. 2007;29(5):834-860. doi: 10.1183/09031936.00112606.

19. Araujo BB, Dolhnikoff M, Silva LF, et al. Extracellular matrix components and regulators in the airway smooth muscle in asthma. *Eur Respir J*. 2008;32(1):61-69. doi: 10.1183/09031936.00147807.

20. Lambert RK, Wiggs BR, Kuwano K, Hogg JC, Pare PD. Functional significance of increased airway smooth muscle in asthma and COPD. *J Appl Physiol*. 1993;74(6):2771-2781.

21. Parameswaran K, Willems-Widyastuti A, Alagappan VK, Radford K, Kranenburg AR, Sharma HS. Role of extracellular matrix and its regulators in human airway smooth muscle biology. *Cell Biochem Biophys*. 2006;44(1):139-146. doi: 10.1385/CBB:44:1:139.

22. Janssen LJ, Killian K. Airway smooth muscle as a target of asthma therapy: History and new directions. *Respir Res*. 2006;7:123. doi: 10.1186/1465-9921-7-123.

23. Ali F, Chin L, Pare PD, Seow CY. Mechanism of partial adaptation in airway smooth muscle after a step change in length. *J Appl Physiol*. 2007;103(2):569-577. doi: 10.1152/japplphysiol.00216.2007.

24. Pratusevich VR, Seow CY, Ford LE. Plasticity in canine airway smooth muscle. *J Gen Physiol*. 1995;105(1):73-94.

25. Bosse Y, Sobieszek A, Pare PD, Seow CY. Length adaptation of airway smooth muscle. *Proc Am Thorac Soc*. 2008;5(1):62-67. doi: 10.1513/pats.200705-056VS.

26. de Lanerolle P, Paul RJ. Myosin phosphorylation/dephosphorylation and regulation of airway smooth muscle contractility. *Am J Physiol*. 1991;261(2 Pt 1):L1-14.

27. Gil FR, Zitouni NB, Azoulay E, Maghni K, Lauzon AM. Smooth muscle myosin isoform expression and LC20 phosphorylation in innate rat airway hyperresponsiveness. *Am J Physiol Lung Cell Mol Physiol*. 2006;291(5):L932-40. doi: 10.1152/ajplung.00339.2004.

28. Salinthone S, Tyagi M, Gerthoffer WT. Small heat shock proteins in smooth muscle. *Pharmacol Ther*. 2008;119(1):44-54. doi: 10.1016/j.pharmthera.2008.04.005.

29. Ibitayo AI, Sladick J, Tuteja S, et al. HSP27 in signal transduction and association with contractile proteins in smooth muscle cells. *Am J Physiol*. 1999;277(2 Pt 1):G445-54.

30. Komalavilas P, Penn RB, Flynn CR, et al. The small heat shock-related protein, HSP20, is a cAMP-dependent protein kinase substrate that is involved in airway smooth muscle relaxation. *Am J Physiol Lung Cell Mol Physiol*. 2008;294(1):L69-78. doi: 10.1152/ajplung.00235.2007.

31. Schneider GB, Hamano H, Cooper LF. In vivo evaluation of hsp27 as an inhibitor of actin polymerization: Hsp27 limits actin stress fiber and focal adhesion formation after heat shock. *J Cell Physiol*. 1998;177(4):575-584. doi: 2-1.

32. Tan CY, Ban H, Kim YH, Lee SK. The heat shock protein 27 (Hsp27) operates predominantly by blocking the mitochondrial-independent/extrinsic pathway of cellular apoptosis. *Mol Cells*. 2009;27(5):533-538. doi: 10.1007/s10059-009-0079-y.

33. Gong TW, Fairfield DA, Fullarton L, et al. Induction of heat shock proteins by hyperthermia and noise overstimulation in Hsf1 (-/-) mice. *J Assoc Res Otolaryngol*. 2011. doi: 10.1007/s10162-011-0289-9.

34. Rylander MN, Feng Y, Zimmermann K, Diller KR. Measurement and mathematical modeling of thermally induced injury and heat shock protein expression kinetics in normal and cancerous prostate cells. *Int J Hyperthermia*. 2010;26(8):748-764. doi: 10.3109/02656736.2010.486778.

35. Markov DI, Pivovarova AV, Chernik IS, Gusev NB, Levitsky DI. Small heat shock protein Hsp27 protects myosin S1 from heat-induced aggregation, but not from thermal denaturation and ATPase inactivation. *FEBS Lett*. 2008;582(10):1407-1412. doi: 10.1016/j.febslet.2008.03.035.

36. Kampinga HH, Brunsting JF, Stege GJ, Konings AW, Landry J. Cells overexpressing Hsp27 show accelerated recovery from heat-induced nuclear protein aggregation. *Biochem Biophys Res Commun*. 1994;204(3):1170-1177. doi: 10.1006/bbrc.1994.2586.

37. Mead J. Point: Airway smooth muscle is useful. *J Appl Physiol*. 2007;102(4):1708-9; discussion 1710. doi: 10.1152/japplphysiol.01419.2006.

38. Otis AB. A perspective of respiratory mechanics. *J Appl Physiol*. 1983;54(5):1183-1187.

39. Fredberg JJ. Counterpoint: Airway smooth muscle is not useful. *J Appl Physiol*. 2007;102(4):1709-10; discussion 1710-1. doi: 10.1152/japplphysiol.01419a.2006.

40. Jesudason EC, Smith NP, Connell MG, et al. Peristalsis of airway smooth muscle is developmentally regulated and uncoupled from hypoplastic lung growth. *Am J Physiol Lung Cell Mol Physiol*. 2006;291(4):L559-65. doi: 10.1152/ajplung.00498.2005.

41. Schittny JC, Miserocchi G, Sparrow MP. Spontaneous peristaltic airway contractions propel lung liquid through the bronchial tree of intact and fetal lung explants. *Am J Respir Cell Mol Biol*. 2000;23(1):11-18.

42. Featherstone NC, Jesudason EC, Connell MG, et al. Spontaneous propagating calcium waves underpin airway peristalsis in embryonic rat lung. *Am J Respir Cell Mol Biol*. 2005;33(2):153-160. doi: 10.1165/rcmb.2005-0137OC.

43. Thomson NC, Rubin AS, Niven RM, et al. Long-term (5 year) safety of bronchial thermoplasty: Asthma intervention research (AIR) trial. *BMC Pulm Med*. 2011;11:8. doi: 10.1186/1471-2466-11-8.

44. Cox G. Bronchial thermoplasty for severe asthma. *Curr Opin Pulm Med*. 2011;17(1):34-38. doi: 10.1097/MCP.0b013e3283410ae4.

45. Wu Q, Xing Y, Zhou X, Wang D. Meta-analysis of the efficacy and safety of bronchial thermoplasty in patients with moderate-to-severe persistent asthma. *J Int Med Res*. 2011;39(1):10-22.

46. Castro M, Rubin AS, Laviolette M, et al. Effectiveness and safety of bronchial thermoplasty in the treatment of severe asthma: A multicenter, randomized, double-blind, sham-controlled clinical trial. *Am J Respir Crit Care Med*. 2010;181(2):116-124. doi: 10.1164/rccm.200903-0354OC.

47. Pavord ID, Cox G, Thomson NC, et al. Safety and efficacy of bronchial thermoplasty in symptomatic, severe asthma. *Am J Respir Crit Care Med*. 2007;176(12):1185-1191. doi: 10.1164/rccm.200704-571OC.

48. Cox PG, Miller J, Mitzner W, Leff AR. Radiofrequency ablation of airway smooth muscle for sustained treatment of asthma: Preliminary investigations. *Eur Respir J*. 2004;24(4):659-663. doi: 10.1183/09031936.04.00054604.

49. Michaud G, Ernst A. Counterpoint: Efficacy of bronchial thermoplasty for patients with severe asthma. is there sufficient evidence? not yet. *Chest*. 2011;140(3):576-7; discussion 577. doi: 10.1378/chest.11-1390.

50. Shifren A, Chen A, Castro M. Point: Efficacy of bronchial thermoplasty for patients with severe asthma. is there sufficient evidence? yes. *Chest*. 2011;140(3):573-5; discussion 578. doi: 10.1378/chest.11-1410.

51. Jarrard J, Wizeman B, Brown RH, Mitzner W. A theoretical model of the application of RF energy to the airway wall and its experimental validation. *Biomed Eng Online*. 2010;9(1):81. doi: 10.1186/1475-925X-9-81.

52. Martin N, Pavord ID. Bronchial thermoplasty for the treatment of asthma. *Curr Allergy Asthma Rep*. 2009;9(1):88-95.

53. Asthmatx Inc., Alair Bronchial Thermoplasty System. Patent: P080032. April 27, 2010 .

54. Asthmatx Inc., Bronchial thermoplasty - the procedure. http://www.btforasthma.com. Updated 2010.

55. Miller JD, Cox G, Vincic L, Lombard CM, Loomas BE, Danek CJ. A prospective feasibility study of bronchial thermoplasty in the human airway. *Chest*. 2005;127(6):1999-2006. doi: 10.1378/chest.127.6.1999.

56. Cox G, Miller JD, McWilliams A, Fitzgerald JM, Lam S. Bronchial thermoplasty for asthma. *Am J Respir Crit Care Med*. 2006;173(9):965-969. doi: 10.1164/rccm.200507-1162OC.

57. Cox G, Thomson NC, Rubin AS, et al. Asthma control during the year after bronchial thermoplasty. *N Engl J Med*. 2007;356(13):1327-1337. doi: 10.1056/NEJMoa064707.

58. Asthmatx Inc., Alair Bronchial Thermoplasty System. April 27, 2010.

59. Danek CJ, Lombard CM, Dungworth DL, et al. Reduction in airway hyperresponsiveness to methacholine by the application of RF energy in dogs. *J Appl Physiol*. 2004;97(5):1946-1953. doi: 10.1152/japplphysiol.01282.2003.

60. Brown RH, Wizeman W, Danek C, Mitzner W. Effect of bronchial thermoplasty on airway distensibility. *Eur Respir J*. 2005;26(2):277-282. doi: 10.1183/09031936.05.00006605.

61. Brown RH, Pearse DB, Pyrgos G, Liu MC, Togias A, Permutt S. The structural basis of airways hyperresponsiveness in asthma. *J Appl Physiol*. 2006;101(1):30-39. doi: 10.1152/japplphysiol.01190.2005.

62. Dyrda P, Tazzeo T, Doharris L, et al. Acute response of airway muscle to extreme temperature includes disruption of actin-myosin interaction. *Am J Respir Cell Mol Biol*. 2010. doi: 10.1165/rcmb.2009-0259OC.

63. Dergez T, Lorinczy D, Konczol F, Farkas N, Belagyi J. Differential scanning calorimetry study of glycerinated rabbit psoas muscle fibres in intermediate state of ATP hydrolysis. *BMC Struct Biol*. 2007;7:41. doi: 10.1186/1472-6807-7-41.

64. Kai T, Yoshimura H, Jones KA, Warner DO. Relationship between force and regulatory myosin light chain phosphorylation in airway smooth muscle. *Am J Physiol Lung Cell Mol Physiol*. 2000;279(1):L52-8.

65. Roti Roti JL. Cellular responses to hyperthermia (40-46 degrees C): Cell killing and molecular events. *Int J Hyperthermia*. 2008;24(1):3-15. doi: 10.1080/02656730701769841.

66. Roti Roti JL, Kampinga HH, Malyapa RS, Wright WD, vanderWaal RP, Xu M. Nuclear matrix as a target for hyperthermic killing of cancer cells. *Cell Stress Chaperones*. 1998;3(4):245-255.

67. Roti Roti JL, Turkel N. Heat-shock-induced changes in nuclear protein and cell killing in thermotolerant HeLa cells. *Radiat Res*. 1994;138(2):286-290.

68. Rempp H, Clasen S, Boss A, et al. Prediction of cell necrosis with sequential temperature mapping after radiofrequency ablation. *J Magn Reson Imaging*. 2009;30(3):631-639. doi: 10.1002/jmri.21863.

69. Brace CL. Microwave ablation technology: What every user should know. *Curr Probl Diagn Radiol*. 2009;38(2):61-67. doi: 10.1067/j.cpradiol.2007.08.011.

70. Chang IA, Nguyen UD. Thermal modeling of lesion growth with radiofrequency ablation devices. *Biomed Eng Online*. 2004;3(1):27. doi: 10.1186/1475-925X-3-27.

71. Brace CL. Radiofrequency and microwave ablation of the liver, lung, kidney, and bone: What are the differences? *Curr Probl Diagn Radiol*. 2009;38(3):135-143. doi: 10.1067/j.cpradiol.2007.10.001.

72. Meltz ML. Radiofrequency exposure and mammalian cell toxicity, genotoxicity, and transformation. *Bioelectromagnetics*. 2003;Suppl 6:S196-213. doi: 10.1002/bem.10176.

73. Mertyna P, Hines-Peralta A, Liu ZJ, Halpern E, Goldberg W, Goldberg SN. Radiofrequency ablation: Variability in heat sensitivity in tumors and tissues. *J Vasc Interv Radiol*. 2007;18(5):647-654. doi: 10.1016/j.jvir.2007.02.033.

74. Nikfarjam M, Malcontenti-Wilson C, Christophi C. Focal hyperthermia produces progressive tumor necrosis independent of the initial thermal effects. *J Gastrointest Surg*. 2005;9(3):410-417. doi: 10.1016/j.gassur.2004.07.008.

75. Fuertes MA, Perez JM, Soto M, Menendez M, Alonso C. Thermodynamic stability of the C-terminal domain of the human inducible heat shock protein 70. *Biochim Biophys Acta*. 2004;1699(1-2):45-56. doi: 10.1016/j.bbapap.2003.12.007.

76. Salinthone S, Ba M, Hanson L, Martin JL, Halayko AJ, Gerthoffer WT. Overexpression of human Hsp27 inhibits serum-induced proliferation in airway smooth muscle myocytes and confers resistance to hydrogen peroxide cytotoxicity. *Am J Physiol Lung Cell Mol Physiol*. 2007;293(5):L1194-207. doi: 10.1152/ajplung.00453.2006.

77. Champagne MJ, Dumas P, Orlov SN, Bennett MR, Hamet P, Tremblay J. Protection against necrosis but not apoptosis by heat-stress proteins in vascular smooth muscle cells: Evidence for distinct modes of cell death. *Hypertension*. 1999;33(3):906-913.

78. Pivovarova AV, Chebotareva NA, Chernik IS, Gusev NB, Levitsky DI. Small heat shock protein Hsp27 prevents heat-induced aggregation of F-actin by forming soluble complexes with denatured actin. *FEBS J*. 2007;274(22):5937-5948. doi: 10.1111/j.1742-4658.2007.06117.x.

79. Pivovarova AV, Mikhailova VV, Chernik IS, Chebotareva NA, Levitsky DI, Gusev NB. Effects of small heat shock proteins on the thermal denaturation and aggregation of F-actin. *Biochem Biophys Res Commun*. 2005;331(4):1548-1553. doi: 10.1016/j.bbrc.2005.04.077.

80. Robinson AA, Dunn MJ, McCormack A, dos Remedios C, Rose ML. Protective effect of phosphorylated Hsp27 in coronary arteries through actin

stabilization. *J Mol Cell Cardiol*. 2010;49(3):370-379. doi: 10.1016/j.yjmcc.2010.06.004.

81. Nijhuis EH, Le Gac S, Poot AA, Feijen J, Vermes I. Bax-mediated mitochondrial membrane permeabilization after heat treatment is caspase-2 dependent. *Int J Hyperthermia*. 2008;24(4):357-365. doi: 10.1080/02656730801944914.

82. Nijhuis EH, Poot AA, Feijen J, Vermes I. Induction of apoptosis by heat and gamma-radiation in a human lymphoid cell line; role of mitochondrial changes and caspase activation. *Int J Hyperthermia*. 2006;22(8):687-698.

83. O'Neill KL, Fairbairn DW, Smith MJ, Poe BS. Critical parameters influencing hyperthermia-induced apoptosis in human lymphoid cell lines. *Apoptosis*. 1998;3(5):369-375.

84. Harmon BV, Corder AM, Collins RJ, et al. Cell death induced in a murine mastocytoma by 42-47 degrees C heating in vitro: Evidence that the form of death changes from apoptosis to necrosis above a critical heat load. *Int J Radiat Biol*. 1990;58(5):845-858.

85. VanderWaal R, Malyapa RS, Higashikubo R, Roti Roti JL. A comparison of the modes and kinetics of heat-induced cell killing in HeLa and L5178Y cells. *Radiat Res*. 1997;148(5):455-462.

86. Purschke M, Laubach HJ, Anderson RR, Manstein D. Thermal injury causes DNA damage and lethality in unheated surrounding cells: Active thermal bystander effect. *J Invest Dermatol*. 2010;130(1):86-92. doi: 10.1038/jid.2009.205.

87. Lepock JR, Frey HE, Heynen ML, Senisterra GA, Warters RL. The nuclear matrix is a thermolabile cellular structure. *Cell Stress Chaperones*. 2001;6(2):136-147.

88. Kijowski JM, Mast MG. Thermal properties of proteins in chicken broiler tissues. *J Food Sci*. 1988;53(2):363 - 366.

89. Vega-Warner V, Smith DM. Denaturation and aggregation of myosin from two bovine muscle types. *J Agric Food Chem*. 2001;49(2):906-912.

90. Lepock JR, Frey HE, Rodahl AM, Kruuv J. Thermal analysis of CHL V79 cells using differential scanning calorimetry: Implications for hyperthermic cell killing and the heat shock response. *J Cell Physiol*. 1988;137(1):14-24. doi: 10.1002/jcp.1041370103.

91. Budihardjo I, Oliver H, Lutter M, Luo X, Wang X. Biochemical pathways of caspase activation during apoptosis. *Annu Rev Cell Dev Biol*. 1999;15:269-290. doi: 10.1146/annurev.cellbio.15.1.269.

92. Kumar V, Abbas A, Fausto N, eds. *Robbins and cotran pathologic basis of disease.* 8th ed. Elsevier; 2010.

93. Goldberg SN. Radiofrequency tumor ablation: Principles and techniques. *Eur J Ultrasound*. 2001;13(2):129-147.

94. Galluzzi L, Aaronson SA, Abrams J, et al. Guidelines for the use and interpretation of assays for monitoring cell death in higher eukaryotes. *Cell Death Differ*. 2009;16(8):1093-1107. doi: 10.1038/cdd.2009.44.

95. Saraste A. Morphologic criteria and detection of apoptosis. *Herz*. 1999;24(3):189-195.

96. Nikfarjam M, Muralidharan V, Malcontenti-Wilson C, Christophi C. The apoptotic response of liver and colorectal liver metastases to focal hyperthermic injury. *Anticancer Res*. 2005;25(2B):1413-1419.

97. Mirkes PE, Little SA, Umpierre CC. Co-localization of active caspase-3 and DNA fragmentation (TUNEL) in normal and hyperthermia-induced abnormal mouse development. *Teratology*. 2001;63(3):134-143. doi: 10.1002/tera.1024.

98. Yang Y, Xing D, Zhou F, Chen Q. Mitochondrial autophagy protects against heat shock-induced apoptosis through reducing cytosolic cytochrome c release

and downstream caspase-3 activation. *Biochem Biophys Res Commun*. 2010;395(2):190-195. doi: 10.1016/j.bbrc.2010.03.155.

99. Chin LY, Bosse Y, Jiao Y, et al. Human airway smooth muscle is structurally and mechanically similar to that of other species. *Eur Respir J*. 2010;36(1):170-177. doi: 10.1183/09031936.00136709.

100. Roti Roti JL, Pandita RK, Mueller JD, Novak P, Moros EG, Laszlo A. Severe, short-duration (0-3 min) heat shocks (50-52 degrees C) inhibit the repair of DNA damage. *Int J Hyperthermia*. 2010;26(1):67-78. doi: 10.3109/02656730903417947.

101. Touchette NA, Cole RD. Differential scanning calorimetry of nuclei reveals the loss of major structural features in chromatin by brief nuclease treatment. *Proc Natl Acad Sci U S A*. 1985;82(9):2642-2646.

102. Leguillette R, Zitouni NB, Govindaraju K, Fong LM, Lauzon AM. Affinity for MgADP and force of unbinding from actin of myosin purified from tonic and phasic smooth muscle. *Am J Physiol Cell Physiol*. 2008;295(3):C653-60. doi: 10.1152/ajpcell.00100.2008.

103. Metzger JM, Lin WI, Samuelson LC. Transition in cardiac contractile sensitivity to calcium during the in vitro differentiation of mouse embryonic stem cells. *J Cell Biol*. 1994;126(3):701-711.

104. Sirotkin AV. Effect of two types of stress (heat shock/high temperature and malnutrition/serum deprivation) on porcine ovarian cell functions and their response to hormones. *J Exp Biol*. 2010;213(Pt 12):2125-2130. doi: 10.1242/jeb.040626.

105. Touchette NA, Cole RD. Differential scanning calorimetry of nuclei reveals the loss of major structural features in chromatin by brief nuclease treatment. *Proc Natl Acad Sci U S A*. 1985;82(9):2642-2646.

106. Lee GJ, Roseman AM, Saibil HR, Vierling E. A small heat shock protein stably binds heat-denatured model substrates and can maintain a substrate in a folding-competent state. *EMBO J*. 1997;16(3):659-671. doi: 10.1093/emboj/16.3.659.

107. Mosser DD, Martin LH. Induced thermotolerance to apoptosis in a human T lymphocyte cell line. *J Cell Physiol*. 1992;151(3):561-570. doi: 10.1002/jcp.1041510316.